

OPTICAL FIBER HUMIDITY SENSOR BASED ON  
EVANESCENT WAVE SCATTERING

By

Lina Xu

A Thesis  
Submitted to the Faculty of  
Mississippi State University  
in Partial Fulfillment of the Requirements  
for the Degree of Master of science  
in Physics  
in the Department of Physics and Astronomy

Mississippi State, Mississippi

August 2004

Copyright by

Lina Xu

2004

OPTICAL FIBER HUMIDITY SENSOR BASED ON  
EVANESCENT WAVE SCATTERING

By

Lina Xu

Approved:

---

Wenchao Ma  
Professor of Physics  
(Director of Thesis)

---

David L Monts  
Professor of Physics  
(Committee Member)  
Graduate Coordinator of Department of  
Physics and Astronomy

---

Shiquan Tao  
Research Associate Professor of DIAL  
(Committee Member)

---

Philip B. Oldham  
Dean of the College of Arts and Sciences

Name: Lina Xu

Date of Degree: August 7, 2004

Institution: Mississippi State University

Major Field: Physics

Major Professor: Wenchao Ma

Title of Study: OPTICAL FIBER HUMIDITY SENSOR BASED ON EVANESCENT  
WAVE SCATTERING

Pages in Study: 57

Candidate for Degree of Master of Science

An optical fiber humidity sensor has been devised using a porous sol-gel silica (PSGS) coating as a transducer. Evanescent wave scattering (EWS) in the PSGS coating. PSGS particles are highly hydrophilic and have a strong tendency to absorb water molecules from the surrounding environment. The absorbed water molecules form a thin layer on the inner surface of the pores inside the porous silica and enhance EWS, from which an indicatory signal can be obtained. The humidity sensor presented in this thesis has a fast response, is reversible, low cost, and has a broad dynamic relative humidity range from  $3.6 \times 10^{-6}\%$  to 100% or humidity range from 1.2ppm to 30000ppm. Because of its multiple advantages, including immunity to electromagnetic interference, resistance to corrosive environments, and high sensitivity, this humidity sensor has various applications. In soil moisture sensing, this humidity sensor can avoid the interference caused by compounds in soil water. For electrical transformer moisture sensing, this humidity sensor can avoid the effect of electromagnetic fields.

## DEDICATION

I would like to dedicate this thesis to my family, Dr. Wenchao Ma, Dr. Shiquan Tao and Dr. David L Monts.

## ACKNOWLEDGMENTS

I would like to take this opportunity to express my gratitude to Dr. Wenchao Ma for agreeing to be my major professor. I would like to thank Dr. Shiquan Tao for instructing my research and my thesis and Dr. David L Monts for serving as committee member for this thesis.

## TABLE OF CONTENTS

	Page
DEDICATION.....	ii
ACKNOWLEDGEMENTS.....	iii
LIST OF FIGURES.....	vi
CHAPTER	
I. OVERVIEW.....	1
1.1 Introduction to humidity sensor.....	1
1.1.1 Relative humidity.....	1
1.1.2 Previous humidity sensors.....	2
1.2 Optical fiber sensor.....	5
1.2.1 History and advantages of optical fiber sensor.....	5
1.2.2 Application of optical fiber sensor.....	7
1.2.3 Previous optical fiber humidity sensors research conducted in DIAL optical fiber sensor laboratory.....	8
1.3 Introduction of EWS optical fiber humidity sensor.....	9
1.4 Sol gel chemistry.....	9
1.4.1 Introduction of sol gel silica.....	9
1.4.2 Sol gel process for making porous silica.....	10
1.4.3 Sol gel silica coating.....	12
1.4.4 Characteristics of sol gel silica.....	14
1.4.4.1 Adsorption of sol gel silica.....	14
1.4.4.2 Optical properties of sol gel silica.....	16
1.4.5 Applications of sol gel silica in optical fiber sensor.....	17
II. EXPERIMENTAL SETUP OF CURRENT OPTICAL FIBER HUMIDITY SENSOR.....	19
2.1 Preparing optical fiber bent probe.....	19
2.2 Testing EWS optical fiber humidity sensor in laboratory.....	20
III. MEASUREMENT AND ANALYSIS.....	22
3.1 The evanescent wave in optical fiber.....	22

CHAPTER	Page
3.2 Testing the light scattering in the porous sol-gel silica coating..	24
3.3 Testing the response of the sol gel silica coated bent fiber probe to moisture.....	27
3.3.1 Testing the sol gel silica coating EWS for moisture sensing.....	27
3.3.2 Testing the sol gel silica coating EWS and absorption for monitoring low level moisture content .....	32
3.4 Structure of sol gel silica coating in EWS optical fiber humidity sensing system.....	36
 IV. DESIGN DETAILS OF A PROTOTYPE OPTICAL FIBER HUMIDITY SENSOR.....	 38
4.1 Introduction .....	38
4.2 Principle of the LED circuit.....	39
4.3 Principle of the photodiode circuit.....	40
4.4 A prototype optical fiber humidity sensor .....	41
 V. APPLICATIONS OF OPTICAL FIBER HUMIDITY SENSOR BASED ON EVANESCENT SCATTERING.....	 45
5.1 Application in soil moisture sensing.....	45
5.1.1 Soil moisture information in need .....	45
5.1.2 Problems of existing humidity sensor.....	45
5.1.3 Modification of sol gel silica coated bent probe.....	46
5.1.4 Test and result.....	47
5.2 Application in concrete moisture sensing.....	48
5.2.1 Concrete moisture information in need .....	48
5.2.2 Problems of existing humidity sensor.....	49
5.2.3 Modification of sol gel silica coated bent probe.....	50
5.2.4 Test and result.....	50
 VI. SUMMARY OF PROTOTYPE OPTICAL FIBER HUMIDITY SENSOR.....	 53
 REFERENCES .....	 54

## LIST OF FIGURES

FIGURES	Page
1.1 Mechanical hygrometer .....	3
1.2 Psychrometer.....	4
1.3 Resistive humidity sensor .....	4
1.4 Capacitive humidity sensor.....	5
1.5 Structure of sol gel silica .....	11
1.6 Physical and chemical adsorption of sol gel silica surface.....	15
1.7 Langmuir Isotherm.....	15
1.8 Light transmission of porous silica.....	17
2.1 Experimental setup for testing the optical moisture sensor .....	20
3.1 Optical fiber with sol gel coating.....	22
3.2 Evanescent wave on the interface of sol gel silica coating and fiber-optic core .....	23
3.3 Light intensity of bent probe with and without sol gel coating under certain relative humidity .....	25
3.4 Light intensity guided through bent fiber probe with and without sol gel silica coating.....	27
3.5 Intensity spectrum of light guided through a sol gel silica coated fiber-optic probe to different relative humidity environments .....	29

FIGURES	Page
3.6 dB response of EWS sol gel silica coated bent fiber-optic probe exposed to different relative humidity against wavelength .....	29
3.7 Calibration curve for quantitative determination of humidity .....	30
3.8 Response of a prototype humidity sensor for monitoring humidity change.....	31
3.9 The fast response of the prototype sensor with a changing dry air flow rate .....	32
3.10 Laboratory setup for testing sol gel silica coated optical fiber probe used to monitoring ppm level water in gas steam.....	33
3.11 Response of sol gel silica coated bent probe to ppm level water concentration.....	35
3.12 Time response of sol gel silica coated bent probe to moisture change on low level moisture content.....	35
3.13 Calibration of low level moisture sensor .....	36
3.14 Sol gel silica coating under electron microscope.....	37
4.1 Schematic of sensor structure .....	37
4.2 LED source driver circuit .....	39
4.3 Photodiode and amplifier, divider circuit .....	40
4.4 Outlook of the current fiber-optic humidity sensor .....	42
4.5 Power supply for the whole electrical circuit .....	43
4.6 Back surface of the whole circuit .....	43
4.7 Front surface of the electrical circuit .....	44
5.1 Calibration curves of sol gel coated probe tested in different time ...	47
5.2 Long term soil moisture monitoring using sol gel silica coated bent optical fiber probe .....	48

5.3	Experiment setup for long term monitoring the moisture in concrete.....	51
5.4	Time response of optical fiber sensor to monitor moisture change in concrete block.....	52

## CHAPTER I

### OVERVIEW

#### **1.1 Introduction to humidity sensor**

Monitoring and controlling gas-phase water content is required in many fields, such as in industries and in daily life. Examples include daily air quality management, weather forecasting, agricultural activity, industrial process control in tobacco production, food processing, oil refinement, metal processing, high purity gas preparation, and semiconductor production, etc. In such varying fields, different applications require different sensors to monitor water concentration in a specific gas environment. For example, a humid air environment (relative humidity from 65% to 70%) is required in a tobacco production line in order to preserve the quality of the tobacco leaves [1]. In such an application, a sensor with sensitivity for detecting water content of x% is appropriate and sufficient. In the microelectronic industry, the performance of many electronic devices can be seriously affected by changes in humidity on the product line [2]. This application needs a more sensitive sensor.

##### *1.1.1 Relative humidity*

Humidity is the amount of water vapor in the air and can be described in different ways including absolute humidity and relative humidity. Absolute humidity is the mass of water vapor contained in a unit volume of air. The term “relative humidity (RH)” is used more often. RH is a measure of actual amount of water in the air as compared with

the amount of water that the air can hold at a certain temperature. At temperature T, RH is expressed by equation (1.1) [3]:

$$RH = \frac{P}{P_g} 100\% \quad (1.1)$$

where P is the partial water vapor pressure, and  $P_g$  is the saturation pressure at temperature T. Partial water vapor pressure is exerted by the water vapor present in the air. The saturation pressure is the maximum partial pressure exerted by the saturated water vapor in the air at a given temperature. Saturation vapor pressure is temperature dependent. The saturation vapor pressure is higher when the temperature is higher. This is because that the kinetic energy of water molecular is greater at higher temperature [4],

$$KE_{ave} = \frac{3}{2} kT \quad (1.2)$$

where  $KE_{ave}$  is the average kinetic energy at temperature T (in Kelvin), and the k is the Boltzmann's constant. When T is higher, more water molecules will escape from the liquid water surface into air, resulting in higher saturation vapor pressure. The relationship between saturation vapor pressure and temperature at 1 atm air pressure can be expressed as [3]

$$P_g = \exp\left(\frac{16.78T - 116.9}{T + 237.3}\right) \quad (1.3)$$

where T is in  $^{\circ}C$ . From Equation (1.1) and (1.3), the ratio of relative humidity  $RH_{at T_1}$  and  $RH_{at T_2}$  at two different temperatures  $T_1$  and  $T_2$  is obtained as follows

$$\frac{RH_{at T_1}}{RH_{at T_2}} = \exp\left(\frac{16.78T_2 - 116.9}{T_2 + 237.3} - \frac{16.78T_1 - 116.9}{T_1 + 237.3}\right) \quad (1.4)$$

The relative humidity change due to temperature change can be computed using Equation (1.4).

### 1.1.2 Previous humidity sensors

#### (1). Mechanical humidity sensors

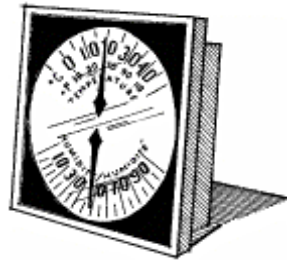


Figure 1.1 Mechanical hygrometer

The mechanical humidity sensor is also known as a hygrometer. It is based on the principle that the change in humidity can be measured with the expansion and contraction of organic substances. Human hair, catgut, cow's intestine, textile plastics, etc. are used in hygrometers. A hygrometer as shown in Figure (1.1) is used in measurement where the humidity has obvious changes. A hygrometer is not reliable in long periods of time because organic substances may stick if the humidity does not change for a long time. It has low sensitivity and can be adversely affected by higher temperature (above 125<sup>0</sup>C) and low relative humidity (below 20%).

#### (2). Wet and dry bulb humidity sensors (psychrometers)

As shown in Figure (1.2), a psychrometer uses the difference in readings between two thermometers, one of which (the dry bulb) is an ordinary glass thermometer, while the other one (wet bulb) has its bulb covered with a clean muslin which is saturated with distilled water prior to observation. When the bulbs are ventilated, they indicate the

thermodynamic wet- and dry-bulb temperatures of the atmosphere. It is precise, reliable and long term stable, but can easily be affected by air flow. It is also difficult to use it at the freezing temperature.

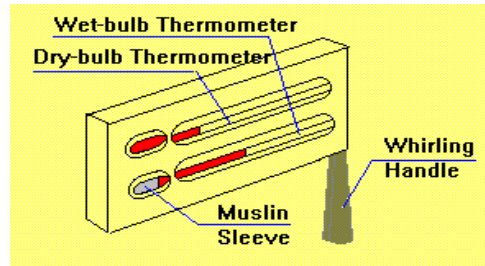


Figure 1.2 Psychrometer

### (3). Resistive humidity sensors

The resistive humidity sensor, as shown in Figure (1.3), is based on the principle of conduction. This sensor's material is sensitive to humidity, and its resistance varies with the change of humidity around it. It is simple and has a fast response, but it is easily contaminated by water soluble salts. Frequent calibration checks are needed for resistive humidity sensors because of their unreliability.

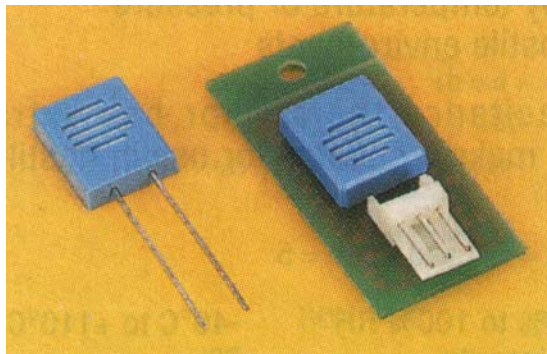


Figure 1.3 Resistive humidity sensors

#### (4). Capacitive humidity sensors

The capacitive humidity sensor, as shown in Figure (1.4), is the most popular humidity sensor among all existing humidity sensors. It is based on the principle of change in the dielectric of a capacitor due to the absorption of the water in the atmosphere. A capacitive humidity sensor consists of a thin layer of polymeric or inorganic material, coated on a conductive base. The layer is then covered with a porous conductive layer. As the humidity increases, the water content of the polymer increases and more charges are stored between the two electrodes. The change of capacitance due to humidity change can be measured.

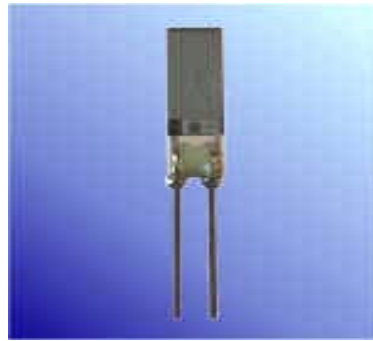


Figure 1.4 Capacitive humidity sensor

## 1.2 Optical fiber sensors

### 1.2.1 History and advantages of optical fiber sensors

People have used light to transmit information for hundreds of years. The invention of laser prompted researchers to study fiber optics for sensing and other applications. Many researchers conducted experiments on optical fiber sensors due to their following advantages over conventional sensors [5]:

(1). Precision and sensitivity: Because of the absence of electrical changes in the transmission of the data through an optical fiber, the optical fiber sensor is immune to electromagnetic disturbance and electrical hazards that affect the measurement accuracy and precision in most conventional electrical sensors. The optical fiber sensor is very sensitive, due to the high sensitivity of its optical response to environmental changes and low signal loss.

(2). Remote sensing: It is possible to use a segment of the fiber as a sensor gauge with a long segment of the same or another fiber conveying the sensing information to a remote station. The optical fiber transmission cables offer significantly lower signal loss, as compared to signal transmission in other conventional sensors, and a high signal-to-noise ratio.

(3). Distributed measurement: An optical fiber communication network allows the user to carry out measurements at different points along the transmission line without much loss when the signal passes through it. This provides an extended method to monitor, control, and analyze the sensed process.

(4). Operation in harsh environment: Fiber optical sensors have been proven to be able to work under extreme conditions, such as high temperature, high pressure, corrosion, toxicity, high radiation, electromagnetically influenced surroundings and other harsh environments.

(5). Compactness and versatility: Optical fibers are intrinsically compact, which helps when building a compact measurement and acquisition system. Furthermore they have been proven to be very versatile due to their ability to perform well in any kind of measurement.

(6). Easy transportation: Since optical fiber cables are very lightweight, it is easy to transport it to any remote place.

### 1.2.2 Applications of optical fiber sensors

Many types of optical fiber sensors based on the change in their optical properties in response to environments have been developed. Optical fiber sensors are categorized mainly into two categories according to their principle of operation: intensity-based sensors and interferometric-based sensors [6]. Intensity sensors measure the change of light intensity guided through the optical fiber. Interferometric sensors sense the phase change of the signal in a sensing fiber as compared to that in a reference fiber. For example, T. Kim *et al.* [7] presented the application of an optical fiber sensor in the measurement of discharging signals by using a Mach-Zehnder interferometry technique.

Optical fiber sensors can also be classified according to their applications: physics sensors, which measure temperature, stress, etc; chemical sensors which measure pH, gas composition, spectroscopic properties, etc; bio-medical sensors which measure blood flow, glucose content, and so on.

K. Newby *et al.* [8] developed a remote optical fiber sensor to collect evanescently excited fluorescence spectra from liquid substances. The sensor is specifically useful for measurement of samples adsorbed from a solution onto the optical fiber sensor. There have been several attempts to measure humidity by optical means [9-23]. Several devices are based on the color change of cobalt chloride that occurs with a variation of humidity [9-12]. Ballantine *et al.* [9] developed an optical fiber humidity

sensor which is incorporated a polymer film containing cobalt chloride. Similarly, Zhou *et al.* [10] demonstrated an optical fiber humidity sensor in which cobalt chloride is applied directly to a porous optical fiber. Wang *et al.* [13] used the changing ultraviolet absorbance of trifluoroacetophenones as the basis for a humidity sensor. Morisawa *et al.* [14] used red-absorbing dyes in Langmuir-Blodgett films for humidity sensing and reported response times of less than 1 s and an effective range between 20 and 80% RH. Sadaoka *et al.* [15] have experimented with a variety of humidity-sensitive dyes dispersed in polymer films. Zhu *et al.* [20] designed an optical fiber humidity sensor utilizing the change in fluorescence intensity of rhodamine 6G entrapped in a Nafion film. Another smart probe design was reported by Mitschke [21]. This design incorporated a humidity-sensitive porous thin-film interferometer on the tip of an optical fiber. Kunz [22] used refractive index changes in an optical waveguide to develop a humidity sensor based on the variable deflection of a laser beam. Otsuki *et al.* [23] reported a humidity sensor based on the opacity change of hydroxypropyl cellulose film in the ultraviolet wavelength range.

### *1.2.3 Previous optical fiber humidity sensors research conducted in the DIAL optical fiber sensor laboratory*

Two types of optical fiber humidity sensors were studied in the Diagnostic Instrumentation Analysis Laboratory (DIAL) optical fiber sensor laboratory. R. Jindal *et al.* [24] developed a fiber optic humidity sensor that was obtained by coating a thin Polyvinyl alcohol (PVA)/CoCl<sub>2</sub> film on a normal optical fiber core. CoCl<sub>2</sub> is a deep blue compound that has a broad absorption spectrum peaked at 690 nm. When CoCl<sub>2</sub> is exposed to humid air, it reacts with water molecules forming a complex Co[H<sub>2</sub>O]<sub>6</sub>Cl<sub>2</sub>,

which is pink. The change in color can be monitored by detecting the light absorption signal of  $\text{CoCl}_2$  or its water complex. S. Tao *et al.*[25] employed an  $\text{CoCl}_2$ -doped fiber as a humidity transducer. The test result showed that the humidity sensor using an active fiber core as transducer has a much higher sensitivity than that of an evanescent-wave based sensor.

### **1.3 Introduction of EWS optical fiber humidity sensor**

An EWS optical fiber humidity sensor belongs to the intensity sensor category. It is based on evanescent wave scattering (EWS) in the porous sol gel silica (PSGS) coating on the surface of a silica optical fiber core. Water molecules in the gas phase surrounding the optical fiber can be adsorbed into the inner surface of the pores inside the sol gel silica. The adsorbed water molecules form a thin liquid layer on the inner surface of the pore and enhance the EWS. The amount of water adsorbed is in dynamical equilibrium with the water vapor pressure in the gas phase. Therefore the humidity in the air can be quantitatively determined with fiber-optic EWS in a PSGS coating.

### **1.4 Sol gel chemistry**

#### *1.4.1 Introduction to sol gel silica*

Sol gel silica is a form of silicon dioxide ( $\text{SiO}_2$ ) with amorphous porous structure. It is formed by the sol gel process. The sol is a colloidal suspension of solid particles in liquid. A gel is a colloid in a more solid form than sol. The sol gel technique was first reported 150 years ago for decorative and constructional materials and was extensively

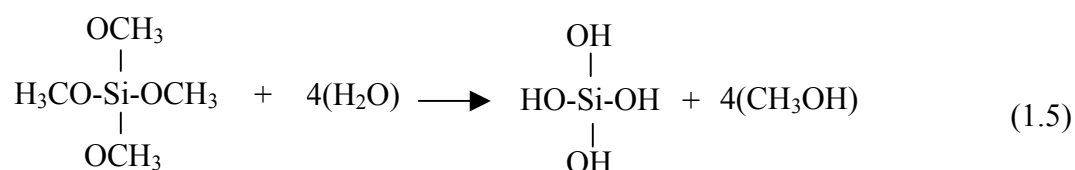
developed in the last century for applications such as glasses, ceramics, catalysts, coating, composites and fibers. It has a number of advantages, such as good purity and homogeneity. D. Avnir *et al* [26] reported that an organic sample could be incorporated in a sol gel glass by adding the organic sample to the sol before gelatinization. This is very important in chemical analysis and optical fiber sensing systems.

#### 1.4.2 Sol gel process for making porous silica

Most sol gel methods employ water and low molecular weight alkoxides, such as tetramethylorthosilicate (TMOS,  $\text{Si}(\text{OCH}_3)_4$ ), tetraethoxysilane (TEOS,  $\text{Si}(\text{OC}_2\text{H}_5)_4$ ), or other organometallic alkoxides, as sol precursors. The process of sol gel formation under room temperature is described below:

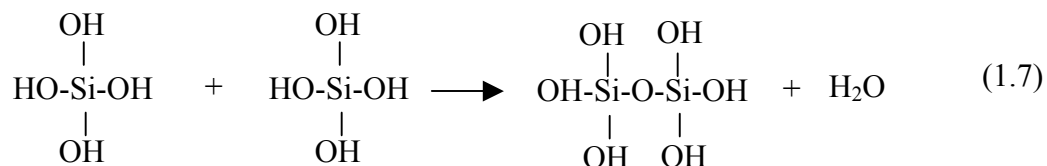
##### (1). Hydrolysis

TMOS is a common precursor that reacts readily with water. The hydrolysis process first substitutes hydrogen ions for methyl groups, which react with hydroxyl ions.



##### (2). Condensation

Two of the partially hydrolyzed molecules can link together in a condensation reaction:



After the condensation reaction, these monomers are able to form a complex branching network by the mechanism of polymerization [27-29].

### (3). Gelatinization

The resulting sol is cast into a mold to form solid gel. This process is called gelatinization.

### 4. Drying and Aging

The expression “drying and aging” is defined as the procedure in which organic solvent escapes or water vaporizes from the pores inside the silica matrix and part of the pores collapse and shrink to form a more compact structure. Typically the volume of the solid matrix shrinks to around 10% of its original volume [30].

In 1934, Hoffman postulated the existence of silanol groups (=Si-OH) on the silica surface [31]. Figure (1.5) shows the structure of sol gel silica.

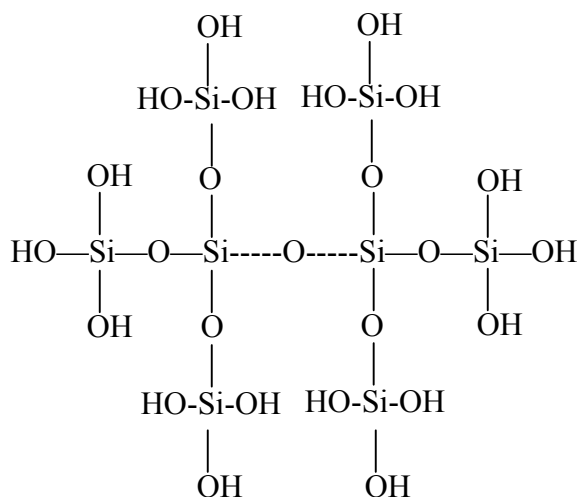


Figure 1.5 Structure of sol gel silica

### 1.4.3 Sol gel silica coating

The two broadly practiced methods of sol gel deposition are dip-coating and spin-coating. In the dip-coating approach, there are six competing forces acting in the film deposition region that determine the position of the streamline which determines the film thickness [32]. Since the sol gel coating with low viscosity is deposited at slow withdrawal speed, the viscous drag and gravity forces are not balanced by the applied film thickness. To properly balance the forces, a modification of the liquid-vapor surface tension,  $\gamma_{LV}$ , is imposed by the liquid-vapor interface, which leads to the following film thickness relationship [33]:

$$h = 0.94(\eta U_0)^{2/3} / \gamma_{LV}^{1/6} (\rho g)^{1/2} \quad (1.8)$$

where  $h$  is the coating thickness,  $\eta$  is the solution viscosity,  $U_0$  is the withdrawal rate,  $\rho$  is the density of the sol, and  $g$  is the gravitational acceleration.

C. G. Brinker *et al.* [34,35] suggested that film formation in sol gel coating is also governed by the competing processes of gravitational draining and solvent evaporation. As the polymeric species are concentrated on the substrate's surface, the processes are accompanied by condensation reactions. Since the drying stage overlaps with the aggregation-gelation stage, there is only a brief time for condensation. Furthermore, there is an added competition between solvent evaporation (which compacts the structure) and condensation (which stiffens the structure). Eventually, compliant structure is collapsed by the capillary pressure created by the liquid-vapor menisci given by the equation

$$P = 2\gamma_{LV} \cos(\theta) / r \quad (1.9)$$

where  $\theta$  is the wetting angle (contact angle of a drop of liquid placed on the surface of the subject object),  $r$  is the pore radius, and  $p$  is the capillary pressure.

Equations 1.8 and 1.9 demonstrate that the properties of the dip-coating film are controlled by the withdrawal rate, the viscosity of the sol, the precursor structure in the sol, and the capillarity of the sol. These conditions permit rearrangement of the silica species upon drying, so that cracking and poor adhesion between the film and the substrate can be avoided.

According to Bornside *et al.* [36], spin-coating is a more dynamic process than dip-coating and can be divided into four stages: deposition, spin-up, spin-off and evaporation. Initially, deposition is the direct addition of the sol to the substrate's surface, usually in excess of the desired coating amount. In the next stage, spin-up causes the excess liquid to flow radially outward, driven by centrifugal forces. During the spin-off stage, liquid flows to the perimeter of the substrate, eventually leaving as droplets. Scriven [37] suggested that the thickness  $h(t)$  of an initially uniform film during spin-off can be by

$$h(t) = \frac{h_0}{(1 + 4\rho\omega^2 h_0^2 / 3\eta)^{1/2}} \quad (1.10)$$

where  $h_0$  is the initial thickness,  $t$  is the time and  $\omega$  is the angular velocity. With a combination of a rise in velocity and film-thinning, however, liquid flow to the edges ultimately diminishes, giving rise to the final stage. As a result, the final solvent evaporates. Collectively the main advantage of spin coating is the film uniformity due to balancing the induced centrifugal forces with the resistant viscosity forces. The time scale of deposition process is greatly reduced because of the increased evaporation rate provided by the increased convection of solvent.

#### 1.4.4 Characteristics of sol gel silica

##### 1.4.4.1 Adsorption of Sol gel silica

Sol gel silica is an amorphous substance with stable chemical properties and has highly complicated porous structure. It is odorless, tasteless, non-toxic, and has high mechanical strength. The most important property that is used in the EWS humidity sensor is sol gel silica's capability of reversible adsorption of gas molecules. The adsorption of gas molecules into a porous material is through the static electric adsorption due to van der Waals force or chemical bond formation. The result is the formation of a gas or liquid film on a solid body. The main water molecule adsorption in the sol gel silica pore is the physical absorption as shown in Figure (1.6).

Several classical adsorption models have been postulated, including Langmiur isotherm, which is suited for monolayer adsorption, Freundlich isotherm, Temkhh isotherm and BET isotherm, which are suited for multilayer adsorption. Langmiur's isotherm (LI) model was used in sol gel silica adsorption because of the fact that if the pore size is around 2-3 nm in porous absorbent, the adsorption isotherm curve still obeys monolayer adsorption isotherm curve [37], although multilayer adsorption exists. The pore diameter inside sol gel silica is just around several nanometers [38]. In the porous sol gel silica matrix, adsorption reaches a dynamical equilibrium in which the liquid evaporates at the same rate as the vapor condenses. Under equilibrium, the LI equation is

$$\theta = \frac{bp}{1 + bp} \quad (1.10)$$

where  $\theta$  is the surface percentage of absorbent site,  $b$  is adsorption coefficient, and  $p$  is the equilibrium pressure.

The LI model is based on three assumptions:

- adsorption cannot proceed beyond monolayer coverage
- all sites are equivalent and the surface is uniform
- the ability of a molecule to be adsorbed at a given site is independent of the occupation of neighbor sites.

Figure 1.7 shows Langmuir isotherm curves with different adsorption coefficients.

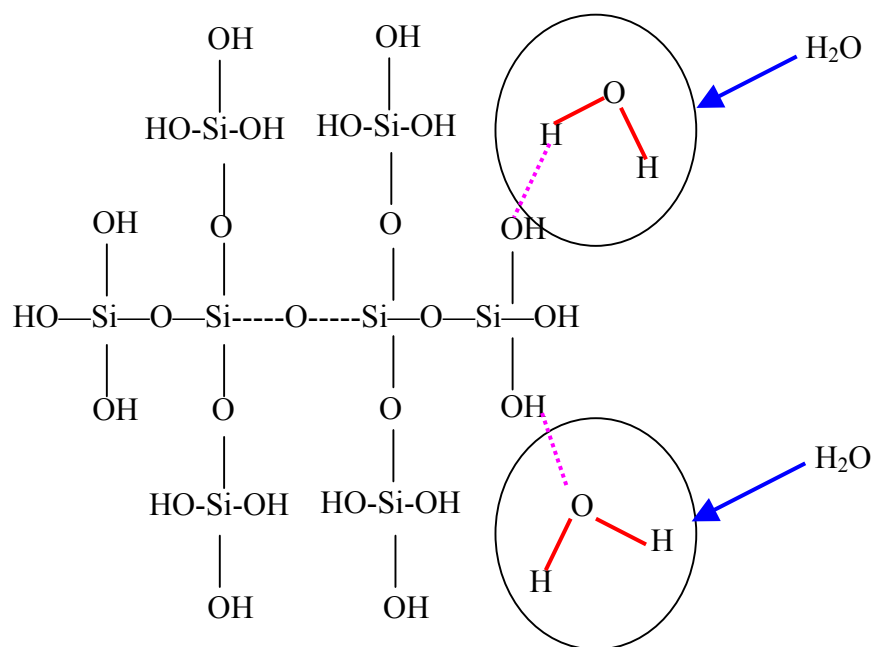


Figure 1.6 Physical adsorption on sol gel silica surface

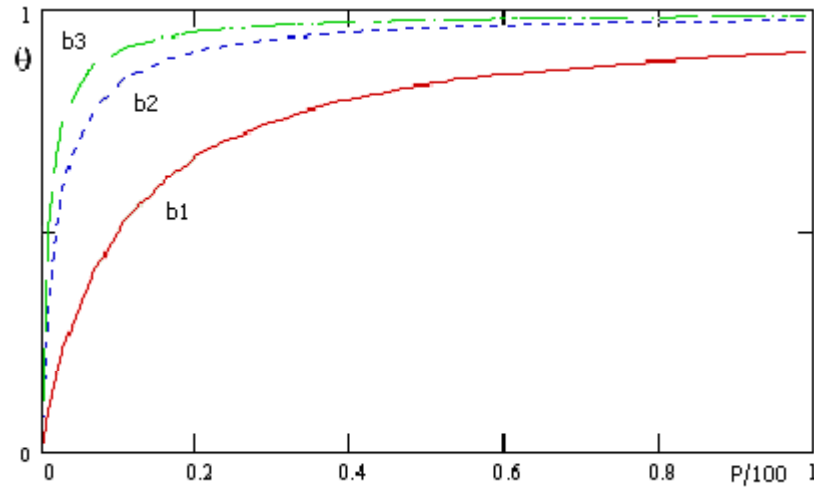


Figure 1.7 Langmuir isotherms with different adsorption coefficients.  $b_3 > b_2 > b_1$

#### 1.4.4.2 Optical properties of sol gel silica

Sol gel silica is transparent to visible and near infrared light as shown in Figure 1.8. In deep the ultraviolet (UV) range, sol gel silica is opaque. Most of the light is scattered out due to Rayleigh scattering. The pores inside sol gel silica act as scattering centers (the actual entity that causes scattering). The scattering centers can be as small as a single large molecule with an inherent inhomogeneity, or clusters of small molecules arranged in a non-uniform way. Rayleigh scattering as a function of wavelength is given by Equation (1.11)

$$T = Ae^{\left(\frac{-C.t}{\lambda^4}\right)} \quad (1.11)$$

where T is transmittance, A is a wavelength independent transmission factor, C is intensity of Rayleigh scattering, t is the sample thickness, and  $\lambda$  is the wavelength. In the

visible and near infrared regions, geometric scattering is prominent because of sol gel silica's amorphous structure. In this region, sol gel silica is an adequate optical material.

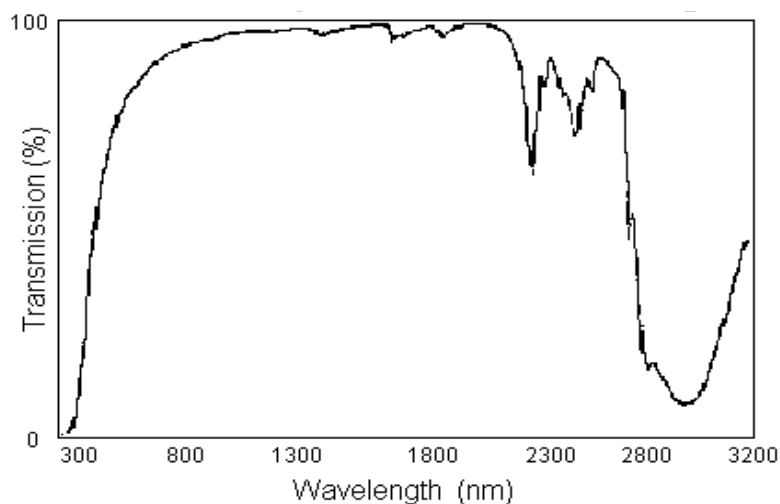


Figure 1.8 The light transmission of porous silica. The transmission in the graph is the fraction of light intensity transmitted through the porous silica [28].

#### 1.4.5 Applications of sol gel silica in optical fiber sensors

Sol gel silica has been used to prepare a number of different sensors. A number of different configurations have been used such as monoliths, films, powders, etc. Ellerby *et al.* [39] showed that the behavior of proteins is very stable in sol gels and the spectroscopic changes of protein in a sol gel matrix are similar to those seen in solution. Kuselman *et al.* [40] designed disposable tube detectors for water analysis using sol gels. A number of optrodes have been designed using the sol gel as a host matrix for the sensor. The first application using sol gels to prepare an optical fiber chemical sensor was proposed in 1989 by Badini *et al.* [41,42], who immobilized fluorescein isothiocyanate in a sol gel glass to sense pH value. In 1991 two different approaches were used to combine optical fiber and sol gel technology to design sensors [42]. Both were pH sensors. In one

of the approaches, the cladding was stripped away from the fiber and the fluorescein-doped sol gel was formed on the fiber core [42]. In the other approach, sol gel silica doped with organic indicators was coated on the porous glass optical fiber made by the chemical method [42]. These applications and many others show that sol gel can be used successfully in the field of optical fiber sensors.

## CHAPTER II

### EXPERIMENTAL SETUP OF EWS OPTICAL FIBER HUMIDITY SENSOR

#### 2.1 Preparing optical fiber bent probe

Two ends of a commercially available optical fiber (300EMT, Thorlab, Inc., Newton, New Jersey) are polished. A small part in the middle of the optical fiber is inserted into a flame to burn off the jacket and the cladding. The resulting optical fiber core portion of the optical fiber is then further bent into a “U” shape while in the flame.

After the optical fiber is cooled to room temperature, the bent part is soaked in a solution of  $K_2Cr_2O_7/H_2SO_4$  for 30 minutes to wash off any organic materials possibly sticking on the surface of the bent part of the fiber. The bent part is then taken out from the solution and rinsed with deionized (DI) water. The bent part of the fiber is further soaked in a 2M NaOH solution for at least 24 hours to activate its surface hydroxyl groups. After rinsing the bent probe with DI water, it is coated with sol gel silica by dipping it into a silica sol solution at least six times to guarantee a coating thick enough for the evanescent wave penetration depth. The coated probe is then kept in a refrigerator over night before use.

The silica sol solution used in this work was made by hydrolyzing TMOS with trace hydrochloric acid as a catalyst. To prepare the sol solution: 2ml of TMOS was mixed with 1ml water (30  $\mu$ l of 0.1M HCl solution was added) for ~5 minutes. A clear

solution was obtained after hydrolysis. This solution was used to coat the bent part of the optical fiber.

## 2.2 Test EWS optical fiber humidity sensor in laboratory

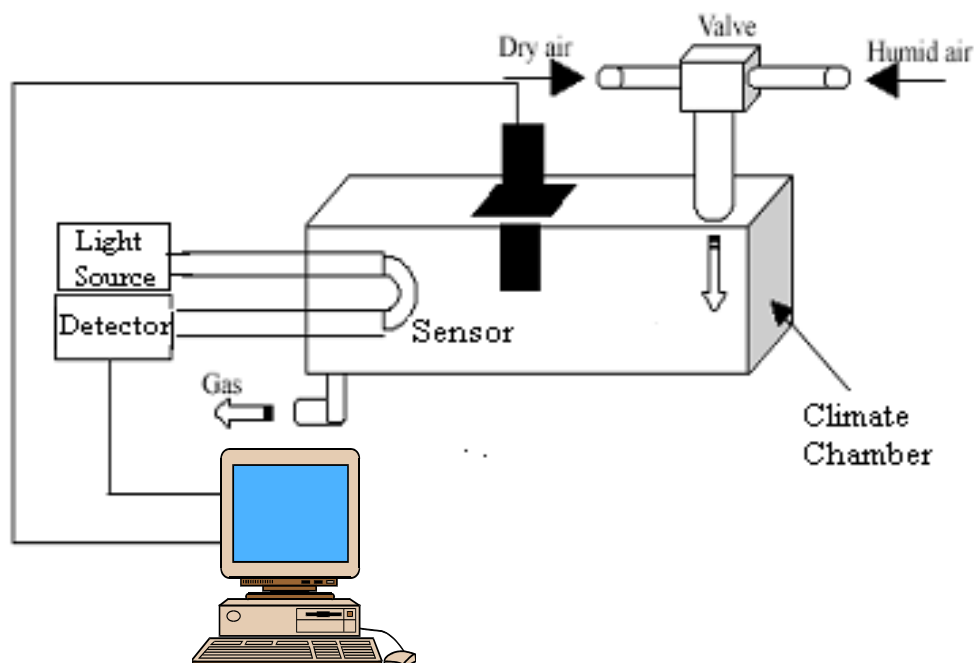


Figure 2.1 Optical fiber humidity sensor experiment setup

Figure 2.1 shows the experimental setup of the fiber-optic humidity sensor. A bent multimode fiber-optic probe was mounted in a simulant climate chamber. The two ends of the optical fiber probe were connected to a broadband light source (DT1000CE, Analytical Instrument System, Inc, Flemington, New Jersey) and an optical fiber compatible UV/V is spectrometer (SD2000, Ocean Optics, Inc, Dunedin, Florida) with SMA connectors, respectively. A commercially available humidity sensor (TRH-100, Pace Scientific, Inc., Mooresville, North Carolina) was also inserted into the chamber to

monitor the RH of the air gas flowing through the chamber. The RH of air through the chamber was controlled by adjusting the flow rate of the dry air and humid air streams. These two gas streams merge before entering the climate chamber.

CHAPTER III  
MEASUREMENTS AND ANALYSIS

**3.1 The evanescent wave in optical fibers**

The sol gel silica coated on the fiber optical core as shown in Figure 3.1 has a refractive index of 1.45 [38], and the refractive index of the fiber optical core is 1.47 (300EMT optical fiber, Thorlabs Inc). According to Snell's law  $\sin \theta = \frac{n_2}{n_1}$ , if the incident angle of a plane wave is greater than the critical angle  $\theta_c$  ( $\theta_c = \sin^{-1}(\frac{n_1}{n_2})$ ) and the light is incident from the material with the higher refractive index to the material with the lower refractive index, total internal reflection occurs. Optical fiber core and the sol gel silica satisfy the requirement of total internal reflection.

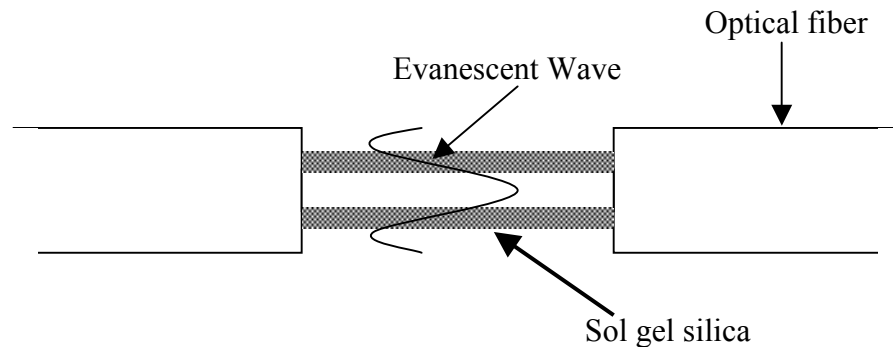


Figure 3.1 Evanescent wave in an optical fiber with sol-gel silica coating

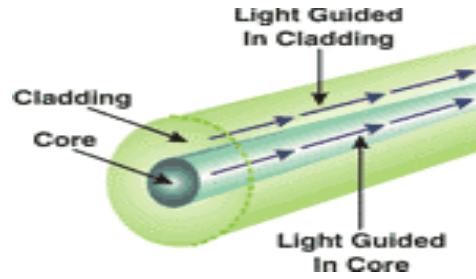


Figure 3.2 Evanescent wave on the interface of sol-gel silica and the fiber optical core

When light travels through a fiber, total internal reflection produces an “evanescent wave” on the interface between the fiber core and sol-gel silica, as shown in Figure 3.2. The evanescent wave is a kind of wave tending to vanish along the direction perpendicular to the interface of the two media. In an optical fiber the evanescent wave propagates in the sol gel silica coating parallel to the interface of the fiber core and the sol gel coating. The amplitude of its electric field decays exponentially along the direction perpendicular to the incident plane. The evanescent wave penetrates a certain distance into the sol-gel coating. The penetration depth ( $d_p$ ) describes the distance from the interface to where the intensity of the evanescent field has decreases to  $1/e$  of the initial intensity. Hence the higher the penetration depth, the higher is the sensing signal. The penetration depth depends on the wavelength of the incident light ( $\lambda$ ), the refractive indices of the fiber core ( $n_1$ ) and the sol gel coating ( $n_2$ ), and the angle of incidence ( $\theta$ ) according to the relationship:

$$d_p = \frac{\lambda}{2\pi\sqrt{n_1^2 \sin^2 \theta - n_2^2}} \quad (2.1)$$

The amplitude of the electrical field  $E(x)$  of the evanescent wave is given

$$E(x) = E_0 \exp\left(-\frac{z}{d_p}\right) \quad (2.2)$$

where  $E_0$  is the initial intensity, and  $z$  is the distance to the interface.

According to S. K. Khijwania and B.D. Gupta [43], the sensitivity of the fiber optic evanescent field absorption sensor based on a U-shaped probe increases with the decrease in the bending radius of the probe. The increment occurs up to a certain value of the bending radius which depends on the fiber numerical aperture and core diameter. Therefore a U-shape bent probe was used in the current experiments.

### **3.2 Testing the light scattering in the porous sol-gel silica coating**

Light scattering is a complex phenomenon and has been observed for a long time. This phenomenon can be used to determine the size of particles, such as aerosols in gas, colloids or micelles in solution, proteins in biological fluids, etc. Therefore light scattering has been widely used for investigation of air pollution, characterization of polymers and colloids, and the study of proteins. Light scattering may be classified into two categories [44]:

- Surface scattering: It is created by interface roughness that maybe due to substrate or material effects.

- Volume scattering: It is created by inhomogeneities in the refractive index that may or may not uniformly distributed. For a uniform distribution, we consider slight continuous random variations in the refractive index, while for nonuniform distributions we have discontinuities connected with the presence of local defects. Because of its porous structure, sol gel silica has a nonuniform distribution in refractive index, producing volume scattering inside.

We tested the evanescent wave scattering phenomenon on bent optical probes with and without sol gel coating under the same conditions, as shown in Figure 3.3. Light intensity guided through the bent probe with a sol gel silica coating has an obvious difference with the intensity guided through the optical fiber without a sol gel silica coating. The light intensity loss in the sol gel silica coated bent probe was caused by evanescent wave scattering. This test was done over the whole visible light range. It also illustrated that sol gel silica has no absorption in visible light.

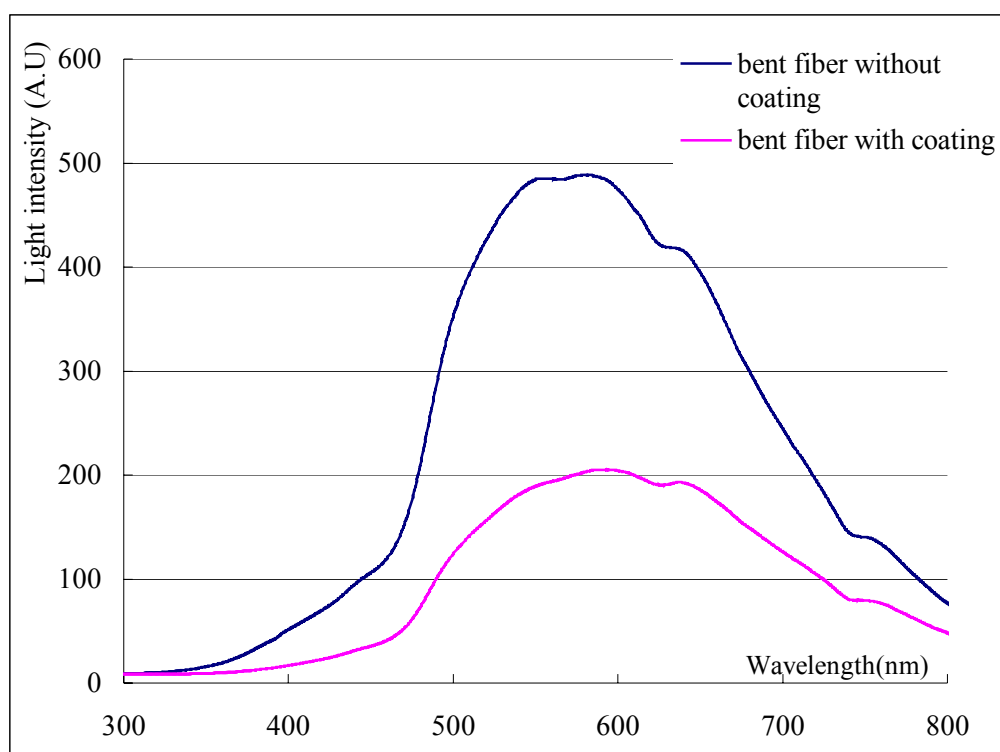


Figure 3.3 The light intensity of bent probe with and without sol gel silica coating under certain relative humidity.

When light is guided through the optical fiber and the evanescent light penetrates into the sol gel silica coating, surface and volume scattering should occur in the sol gel silica layer, because of the porous sol gel silica's structure. Scattering occurs so many

times that the phases of the scattered fields were completely randomized and only the intensity of the light can be considered. These phenomena verified that evanescent scattering occurs in the sol gel silica coating.

According to Langley *et al.* [45], the light scattering phenomenon observed in such porous material is analyzed by using diffusing-wave spectroscopy. In a simplified backscattering model, the scattering light intensity Equation is expressed as:

$$I_E = \exp(-k\gamma\lambda) \quad (3.1)$$

where  $\gamma$  is proportional to the reciprocal of the mean free path length (average distance a ray travels before it encounters an obstacle and reflects) of light propagation in porous material,  $\lambda$  is the wavelength of light, and  $k$  is a constant. This equation indicates that the scattered light intensity is proportional to the negative exponent of wavelength. The dependence of the scattering on the wavelength is also observed in EWS optical fiber humidity experiment as shown in Figure 3.4.

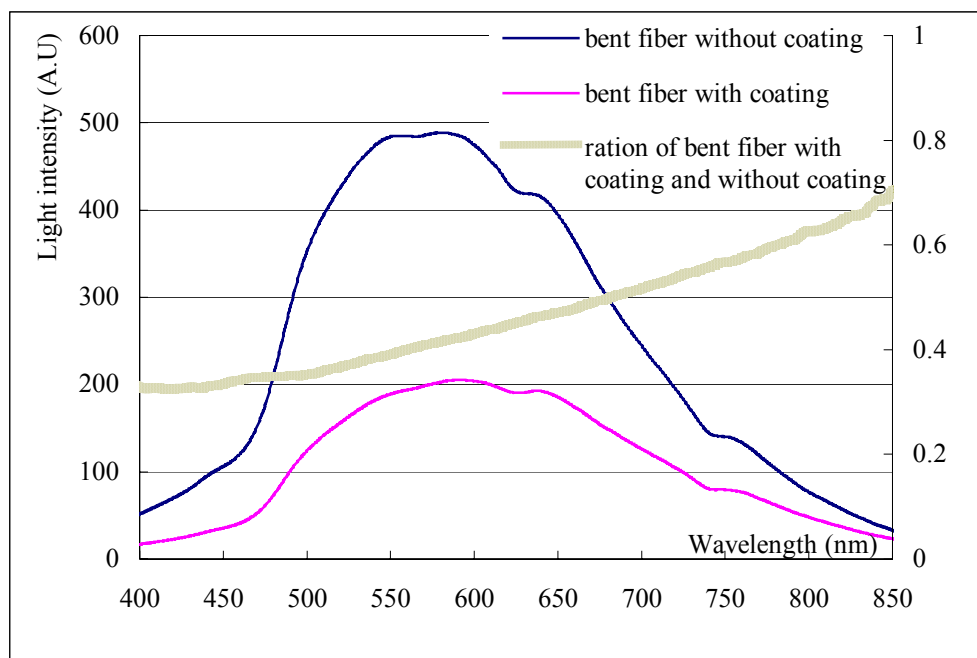


Figure 3.4 Light intensity guided through bent fiber with and without sol gel silica. The right coordinate is the transmission coefficient, from the thick curve we observe that the longer the wavelength, the higher the transmission coefficient

### 3.3 Testing the response of the sol gel silica coated bent fiber probe to moisture

#### 3.3.1 Testing the sol gel silica coating EWS for moisture sensing

The pore surface of sol gel silica is hydrophilic and has a strong tendency to absorb water molecules from the gas phase through hydrogen bond formation. The absorbed water molecules form a layer of liquid water on the surface of the pore walls. Therefore, there are three phases (solid sol gel silica, liquid water and air gas) inside the porous sol gel silica. When a light beam is guided through such a porous material, the light is diffused first in the solid-liquid interface and again in the liquid-gas interface. With a higher humidity in the gas environment around such a material, more water

molecules are absorbed into the inner surface of the pores and a thicker liquid film is formed on the inner surface of the pores. This thicker film increases the free path length of light propagation in the liquid phase and thus enhances the light scattering in the liquid-gas interface [45]. The guided light intensity of the sol gel silica coated bent probe in air gas of different moisture contents was tested and the results are presented in Figure 3.5. With an increase of the relative humidity, the light intensity guided through the probe decreased in the entire range of wavelengths.

Taking the total transmitted light intensity at 3% relative humidity( 3% relative humidity is the lowest relative humidity we obtained in this experiment) as the maximum guided intensity. The attenuation of light intensity expressed in decibels (dB) is calculated as follows:

$$dB = 10 \times \log(I_{3\%RH} / I) \quad (3.2)$$

where  $I_{3\%RH}$  is the light intensity at 3% relative humidity, and  $I$  is the light intensity when the probe is exposed to a sample gas. The relationship of dB versus wavelength at different humidity values is plotted in Figure 3.6. It also shows that the response of this sensor to moisture change is independent of the wavelength of light guided through the optical fiber.

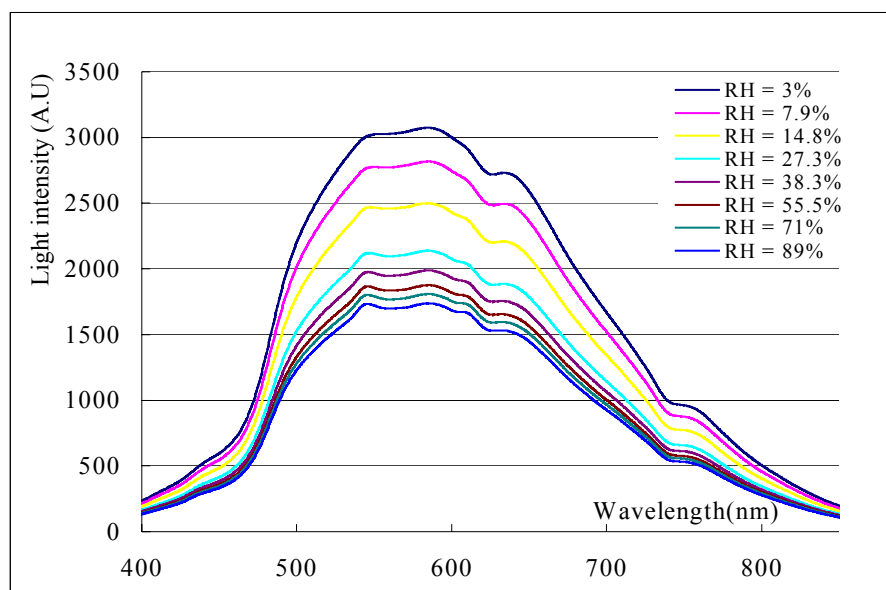


Figure 3.5 Intensity spectra of light guided through a sol gel silica coated optical fiber probe exposed to different relative humidity environments. The bottom curve demonstrates RH=3%, the second curve from bottom demonstrates RH=7.9%, and so on.

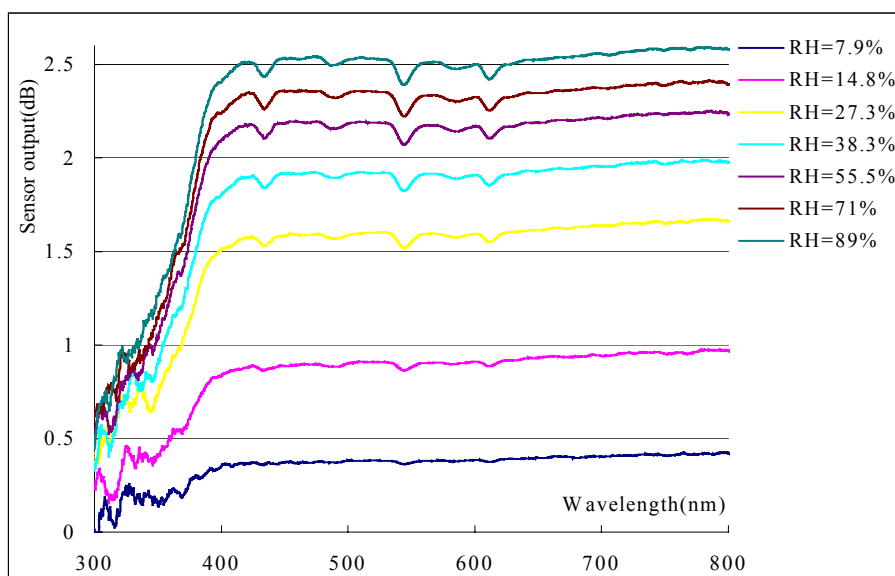


Figure 3.6 The dB response of sol gel silica coated bent fiber probe to air gas of different humidity against wavelength. The small spikes at around 430, 540, and 610nm are caused by light from mercury fluorescence illuminating lamp in the laboratory. The light from the mercury lamp was coupled into the optical fiber probe through scattering by PSGS coating.

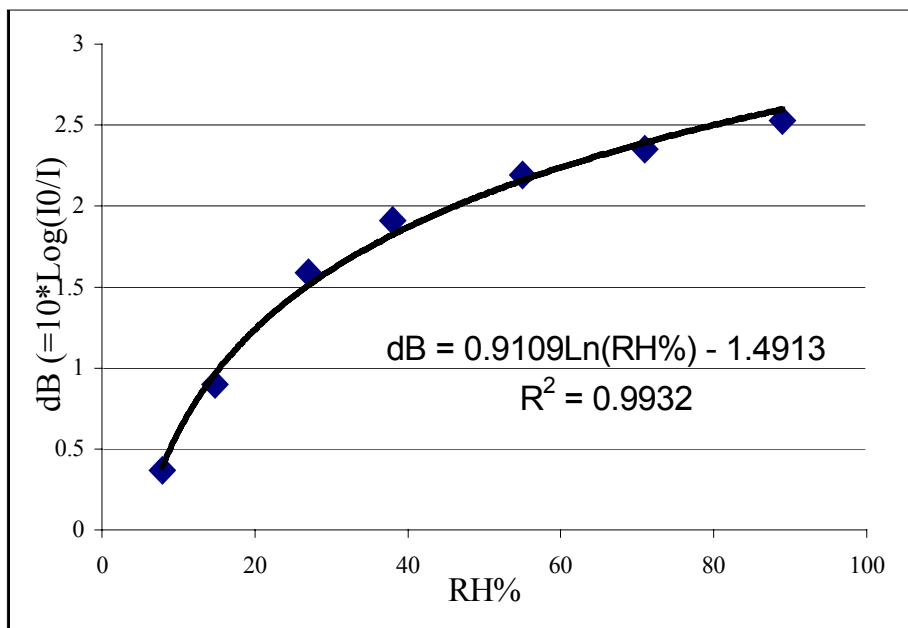


Figure 3.7 Calibration curve for quantitative determination of humidity with sol gel silica coating on the bent probe. dB is defined as  $dB=10*\log(I_{RH=3\%} / I_{RH})$ .

The calibration on relationship of the sensor output in dB as a function of relative humidity is presented in Figure 3.7. This calibration curve follows a Langmuir isotherm adsorption isotherm. This indicates the output of sensor is proportional to the amount of water adsorbed into the coating.

The time response of the sensor for sensing relative humidity is presented in Figure 3.8. Figure 3.9 shows part of the time response from 9200s to 9250s and it coincides with the spike in Figure 3.8. This spike was caused by suddenly changing the dry air flow rate. Compared with commercial humidity sensors, the prototype sensor has a fast response time, and detected the swift change while commercial humidity sensors can not detect this fast event

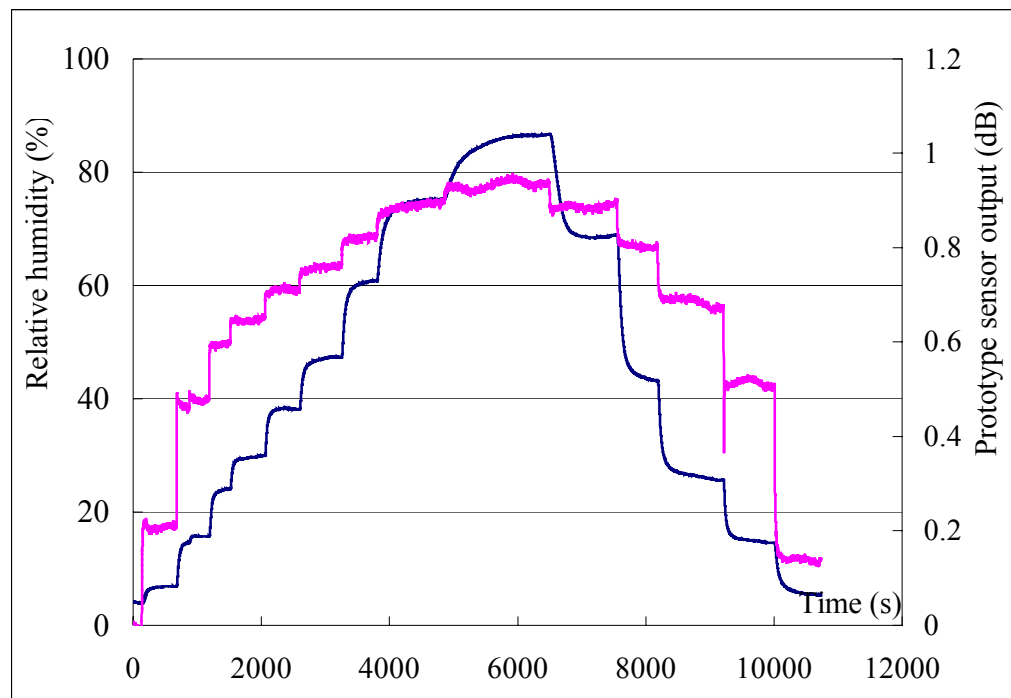


Figure 3.8 Time response of prototype humidity sensor for monitoring humidity change. Prototype sensor output dB in this graph is defined as  $\text{dB} = 10 \cdot \log(I_{\text{RH}=5\%} / I_{\text{RH}})$ . The spike of prototype sensor response at 9369 s is caused by a fast change in the dry air flow rate.

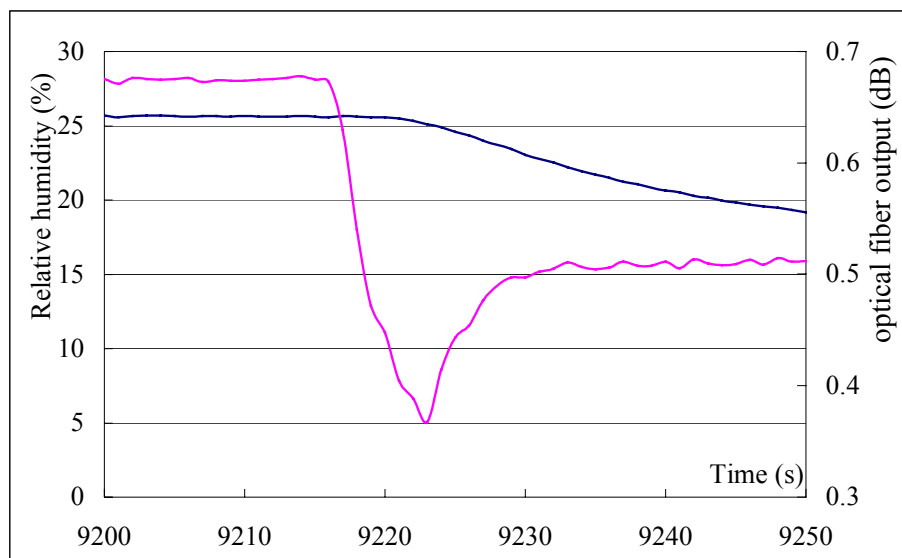


Figure 3.9 The fast response of prototype sensor with a changing dry air flow rate. It coincides with the spike in Figure 3.8

### 3.3.2 Testing the sol gel silica coating EWLS and absorption for monitoring low level moisture content

Monitoring and controlling ultra-low moisture content plays very important roles in industry. Most of the large transformers in power distribution network require very low moisture content [46]. S.M. Fine *et al.* [47] investigated the effect of moisture content of HBr on semiconductor product line. Water molecules need to be removed from natural gas to prevent corrosion, gas hydrate formation, condensation, and freeze-up in the pipeline. The sensor of this study was developed for sensing ppm (particle per million) level water in dry air gas. The test system was built as shown in Figure 3.10.

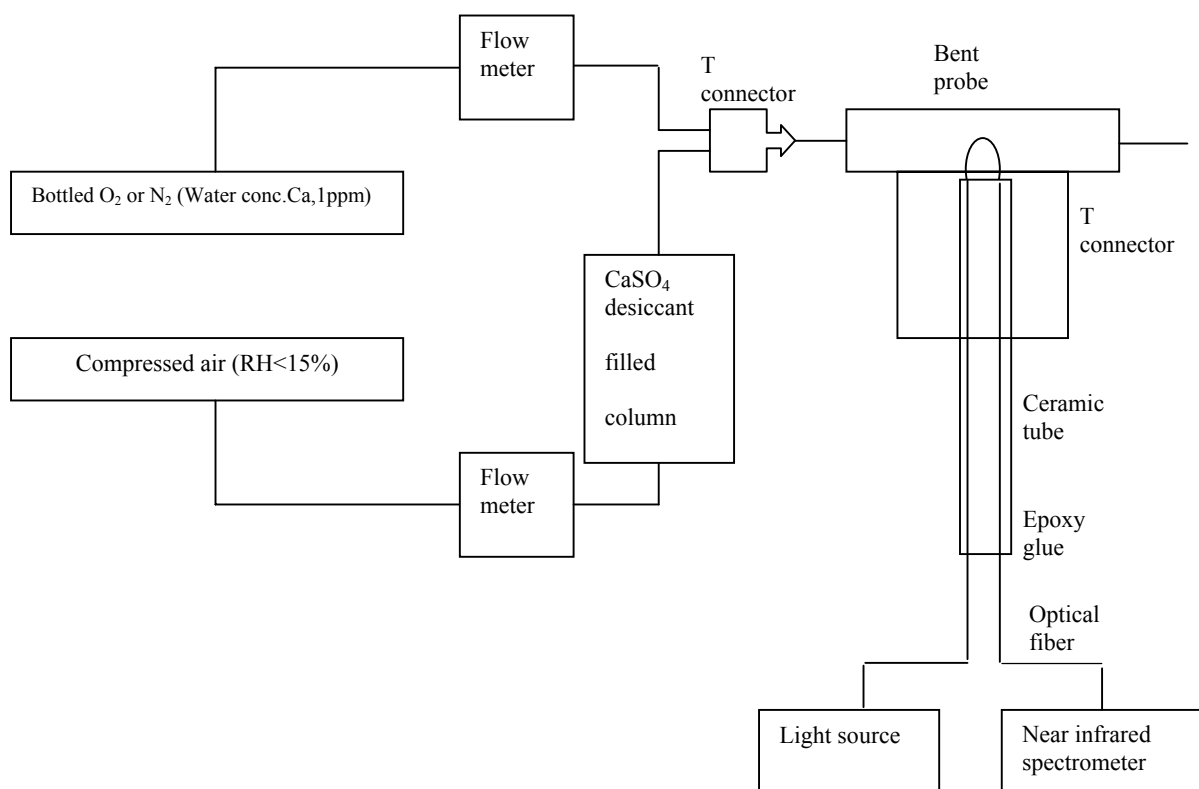


Figure 3.10 Block Diagram of laboratory setup for testing sol gel silica-coated optical fiber probe used to monitor ppm level water in gas steam.

Sample gas contained water in ppm levels is obtained by diluting "dry air" gas with bottled pure nitrogen or oxygen gas, purchased from Airgas. Inc. The concentration of water in the bottled pure gas is <1 ppm (data from gas supplier, Airgas. Inc). The "dry air" gas is obtained by flowing compressed air (RH<15%) through a desiccant (CaSO<sub>4</sub>) filled column. Water concentration in air gas in equilibrium with the desiccant is 6 ppm (date from the desiccant supplier, W.A. Hammond Drierite Co. LTD). The two gas lines were mixed in a T-connector and the obtained mixed gas was used as the sample. The sample gas flows through another T-connector inside which the optical fiber humidity sensor of this work is inserted and sealed, as shown in Figure 3.10. The light source used

in this test is a halogen/tungsten lamp which gives strong emission from the visible to the near infrared (NIR) range. An optical fiber-compatible NIR spectrometer is used as the wavelength-selective detector. The benefit of using the NIR spectrometer to observe the spectrum of light guided through the moisture sensor probe is that the evanescent wave absorption of water molecules inside sol gel silica coating can be observed.

Test results are shown in Figures 3.11 to 3.13. Figure 3.11 shows the spectra response of the sensor to the “dry air ” gas diluted with bottled oxygen gas. Water concentration in the sample gas varies from 1 ppm (oxygen) to 6 ppm (“dry air”). With increased moisture content, the light intensity decreased in the whole region. This demonstrates that evanescent wave scattering does occur. At 1900nm, there is an absorbance peak caused by water molecules’ evanescent wave absorption.

Figure 3.12 shows the time response of the sensor to the change of water concentration in the oxygen-diluted “dry air”. This figure indicates the noise level, response time and reversibility of the sensor to the air gas with a low water concentration from 1ppm to 6 ppm.

Figure 3.13 shows the calibration of the sensor response to the air gas with low water concentrations. The result suggests that sol gel silica’s adsorption of water vapor in the low water concentration region also follows the Langmuir isotherm which is similar to that in the high water concentration region (RH from 4% to 90%).

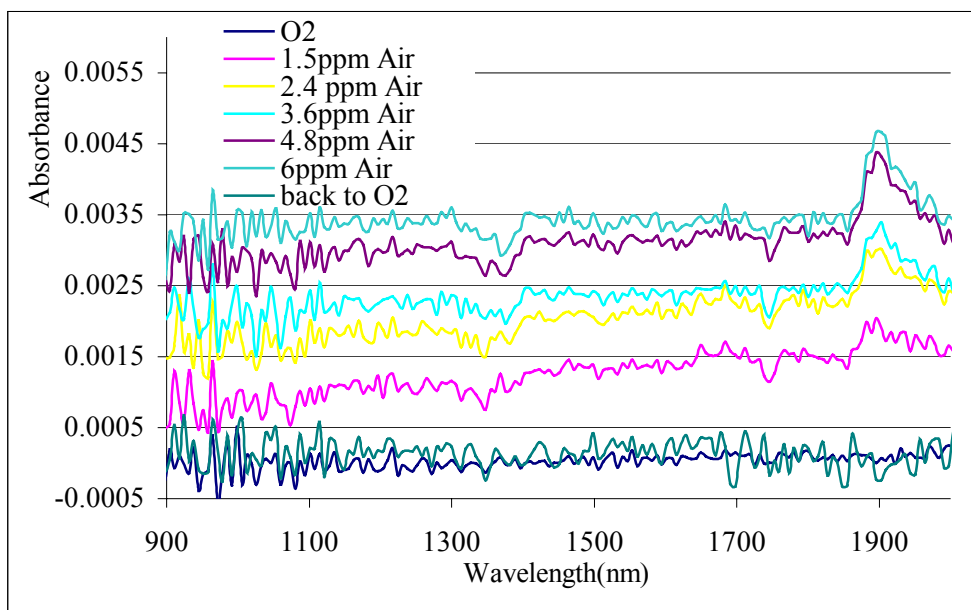


Figure 3.11 Response of bent fiber optical probe with sol gel silica coating to ppm level moisture content.

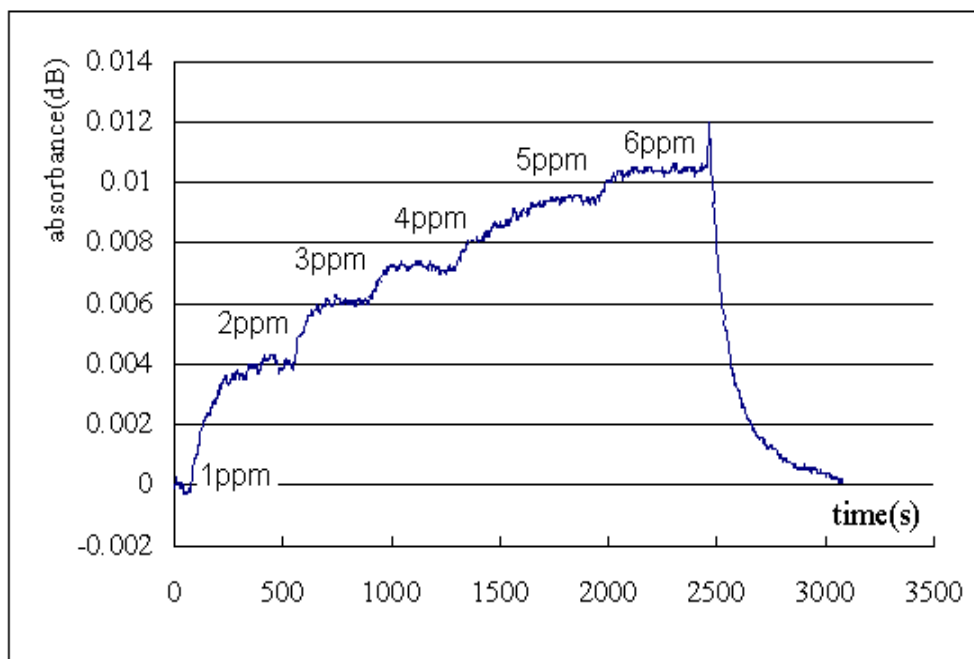


Figure 3.12 Time response of bent fiber optical probe to changes of low level moisture content

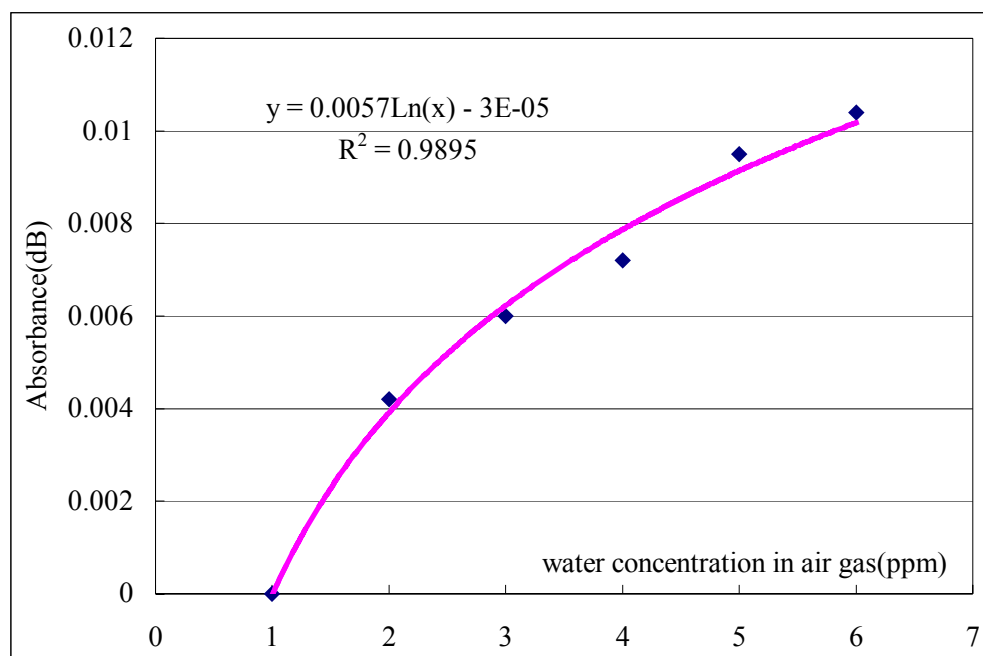


Figure 3.13 Calibration of ultra low level moisture sensor

### 3.4 Structure of sol gel silica coating in current optical fiber humidity sensing system

The sol gel method and the coating method used in this research are discussed in previous chapters. The structure of sol gel silica coating on a normal optical fiber core is shown in Figure 3.14. In the bottom part, some pores can be seen clearly. On the top, some cracks were created by shrinking during the drying process discussed in Chapter 1, and the vacuum environment in the scanning electron microscope cabin. Water molecules are not only absorbed on the inner surface of the pores inside the sol gel silica, but also on the cracked surface because sol gel silica's surface hydroxyl groups attract water molecules. This results in scattering in the pores and cracked surface at the same time.

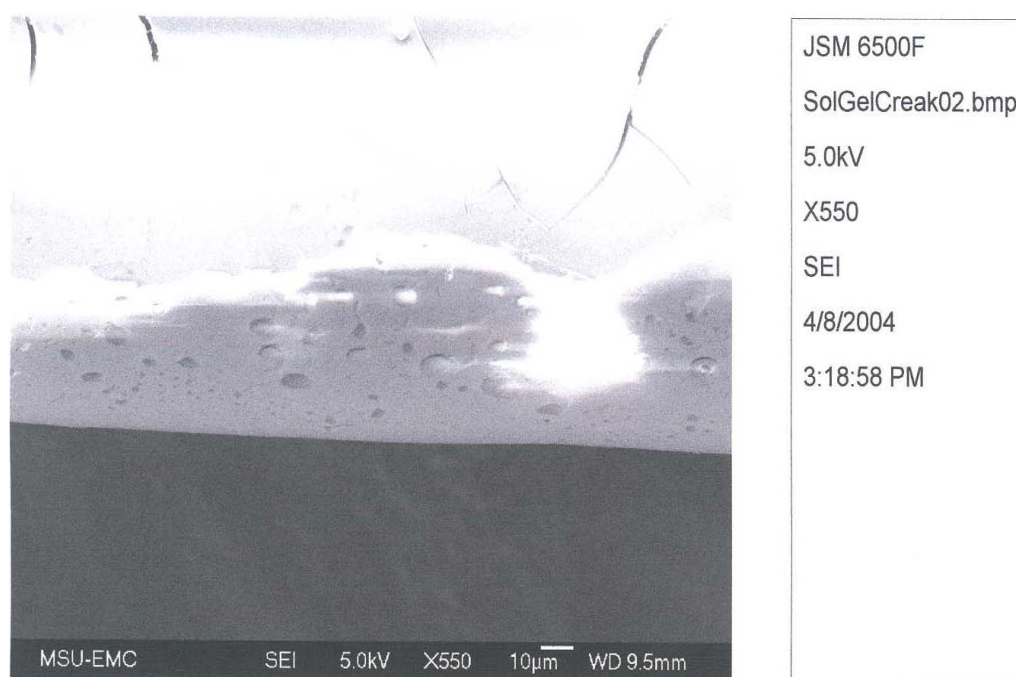


Figure 3.14 Sol gel silica coating under electron microscope showing cracks and porous structure. The crack came from the shrinkage during gelatinization and interaction between atoms. The upper part has no pores because the thickness of coating is thinner than the sol gel silica pore size.

## CHAPTER IV

### DESIGN DETAILS OF A PROTOTYPE OPTICAL FIBER HUMIDITY SENSOR

#### 4.1 Introduction

As described in previous chapters, the response of a PSGS-coated EWS humidity sensor is independent of the wavelength of light guided through the optical fiber. Therefore, a simple light source, such as a light emitting diode (LED), can be used as the light source. In addition, no dispersing element is needed in this sensor design. Several simple components, including one sol gel-coated optical fiber as transducer, one LED as light source, and one photodiode as detector, can form a prototype sensor as shown in Figure 4.1.

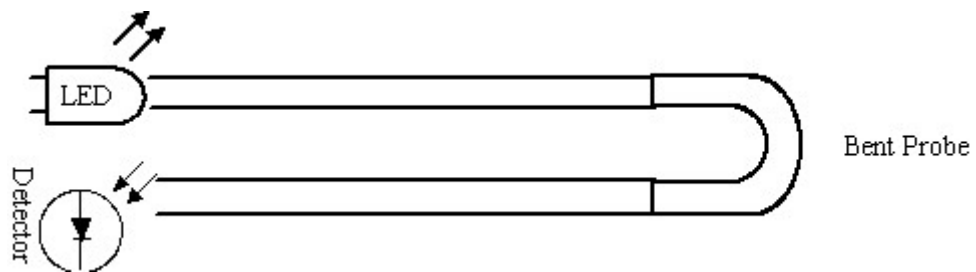


Figure 4.1 Schematic of a prototype sensor structure

## 4.2 Principle of the LED circuit

The LED source is driven by constant electric current as shown Figure 4.5.

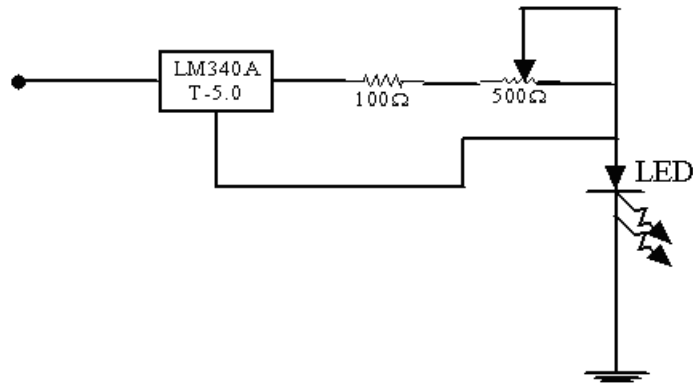


Figure 4.2 The LED source driver circuit

The purpose of the LED driver circuit is to maintain a constant DC current passing through the LED. The LM340 AT-5.0 monolithic 3-terminal positive voltage regulator works under input voltages from 10V to 23V. A standard value of 15V was used as the input voltage in the current LED driver. The regulator outputs a stable voltage of 5V. The current is controlled by the resistors in the circuit based on Equation (4.1).

$$I = \frac{V}{R_1 + R_2} + I_B \quad (4.1)$$

where  $\Delta I_B = 1.3\text{mA}$  over line and load change. This value is smaller as compared to the current going through the LED. The DC current from the LED drive is rather stable. Although a relatively constant current and stable voltage are provided to the LED, the light output from the LED still fluctuates. To avoid this problem, a reference optical fiber with its original coating is connected to the LED, the same as the optical fiber sensor.

### 4.3 Principle of the photodiode circuit

Photodiodes (OPT301M, Texas Instrument) were used to detect the light intensity from the optical fiber bent probe and the reference as shown in Figure 4.5. The photodiodes come with amplifiers inside, which are controlled by the feedback resistors. Capacitors in the circuit are used to filter the noise.

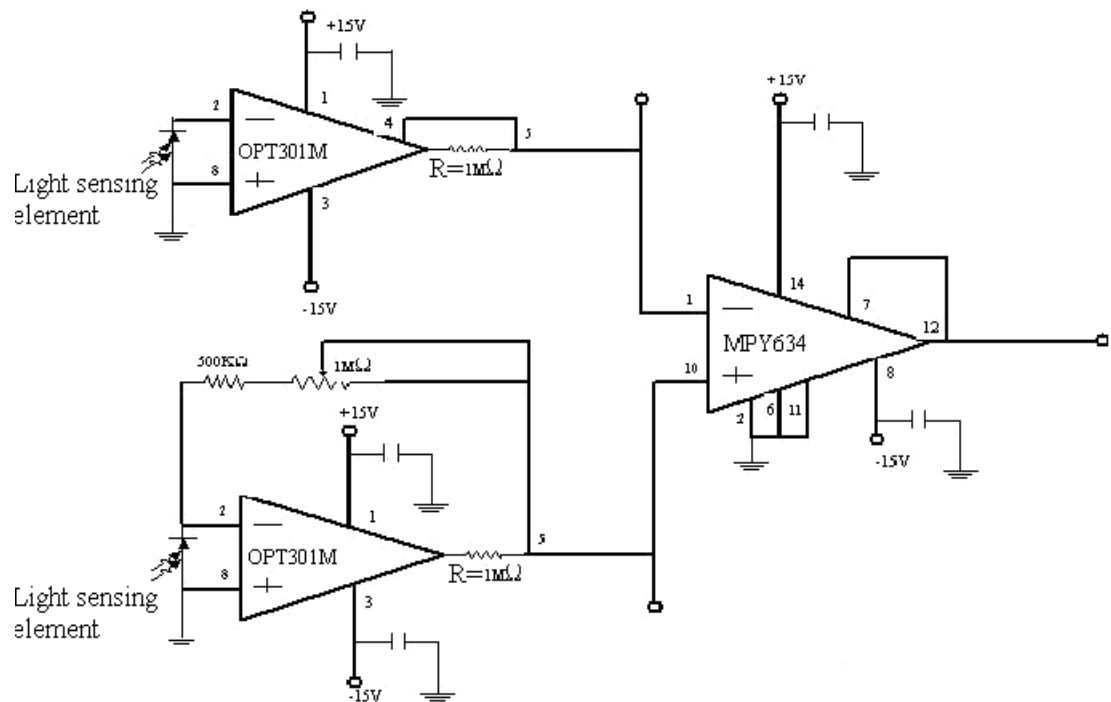


Figure 4.3 Photodiode and amplifier divider circuit.

Every capacitor in the circuit is  $0.1\mu\text{F}$

There are two OPT301M amplifiers, one is used for the fiber-optic sensor, and the other one as the reference to monitor the stability of the LED. The output of the OPT301M connected to the sensor is

$$V_s = I_s * (500k\Omega + R) \quad (4.2)$$

where  $I_s$  is the current produced by the photodiode when the light from, the optical fiber sensor shines on it,  $R$  is an adjustable resistor ranging from 0 to  $1M\Omega$ , and  $500k\Omega$  is from the feedback resistor.

The output of the reference side is

$$V_r = I_r * 1M\Omega \quad (4.3)$$

where  $I_r$  is the current produced by the photodiode when light from reference fiber shines on it. The  $1M\Omega$  is the feedback resistor built in the integrated circuit. A divider (MPY634, Texas Instrument) was used to avoid LED unstable noise in the sensing system. The voltage output of the MPY634 is

$$V = 10 * \frac{V_s}{V_r} \quad (4.4)$$

When LED fluctuates, sensor and reference will fluctuate equally at the same time. The ratio of these two outputs will compensate for the fluctuation.

#### 4.4 A prototype optical fiber humidity sensor

The final humidity sensor system combining the separate circuits together was produced and is shown in Figure 4.4. An optical fiber bent probe and a normal optical fiber which acts as reference, were connected to three SMA connectors on the top of the sensor box. One SMA is connected to the LED light source by two optical fibers. The other two SMA connectors are connected to the sensor and reference separately. A 940nm LED is used to avoid the effect of room light. The output voltage has a linear relationship with the light intensity shining on the photodiode. With the humidity changes, the changes of the output voltage has the same trend as shown in Figure 3.7.

The output signal is directed to a data acquisition card connected to a computer. The software package LabVIEW(National Instruments, Austin, Texas ) is used to process the signal.

Figures 4.5-4.7 show the actual electrical circuits inside the sensor box. Figure 4.5 shows the power supply of the whole circuit. The equipment can be connected directly with 110V AC power. Figure 4.6 and Figure 4.7 show the front surface and the back side of the circuit board of this sensor, which includes the LED driver and the photodiode circuits.



Figure 4.4 Outlook of the electrical part in the fiber optical humidity sensor

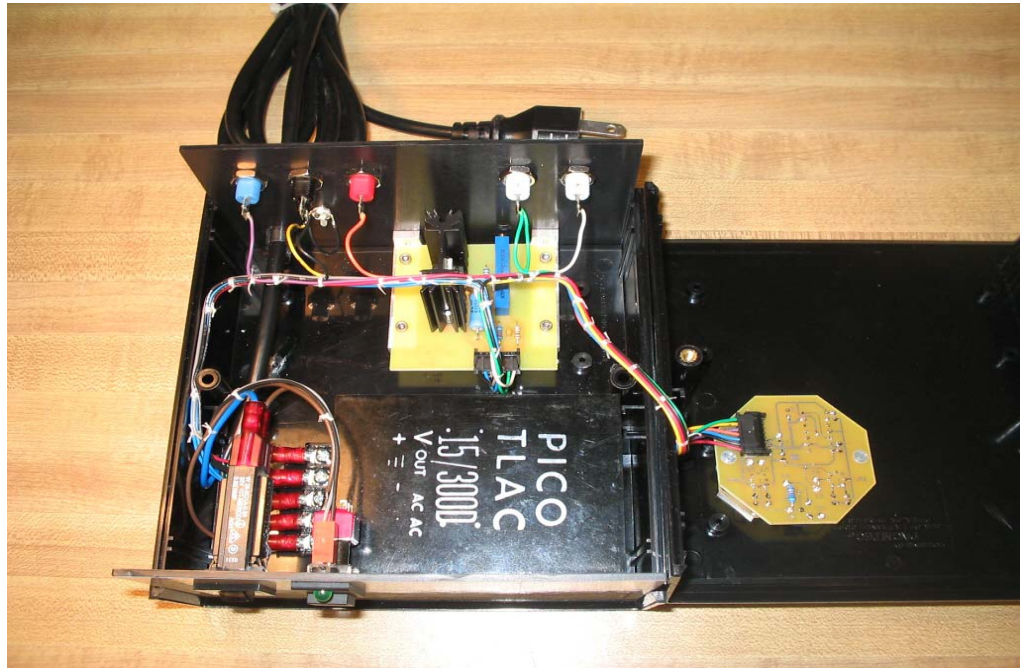


Figure 4.5 Power supply for the whole electrical circuit.

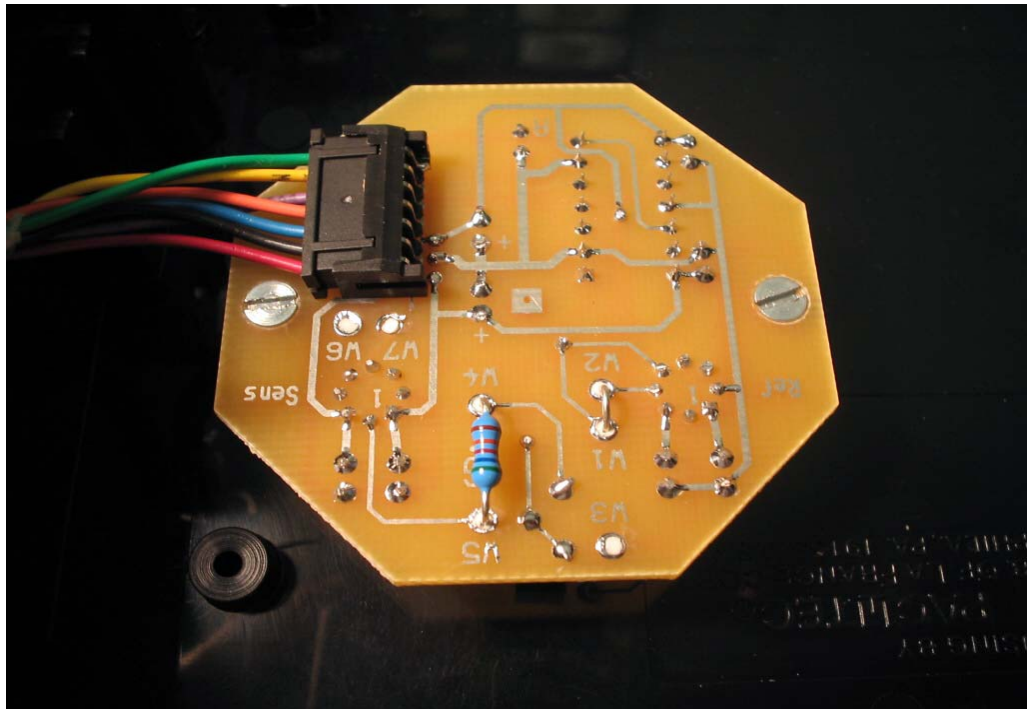


Figure 4.6 Back side of the electric circuit board.

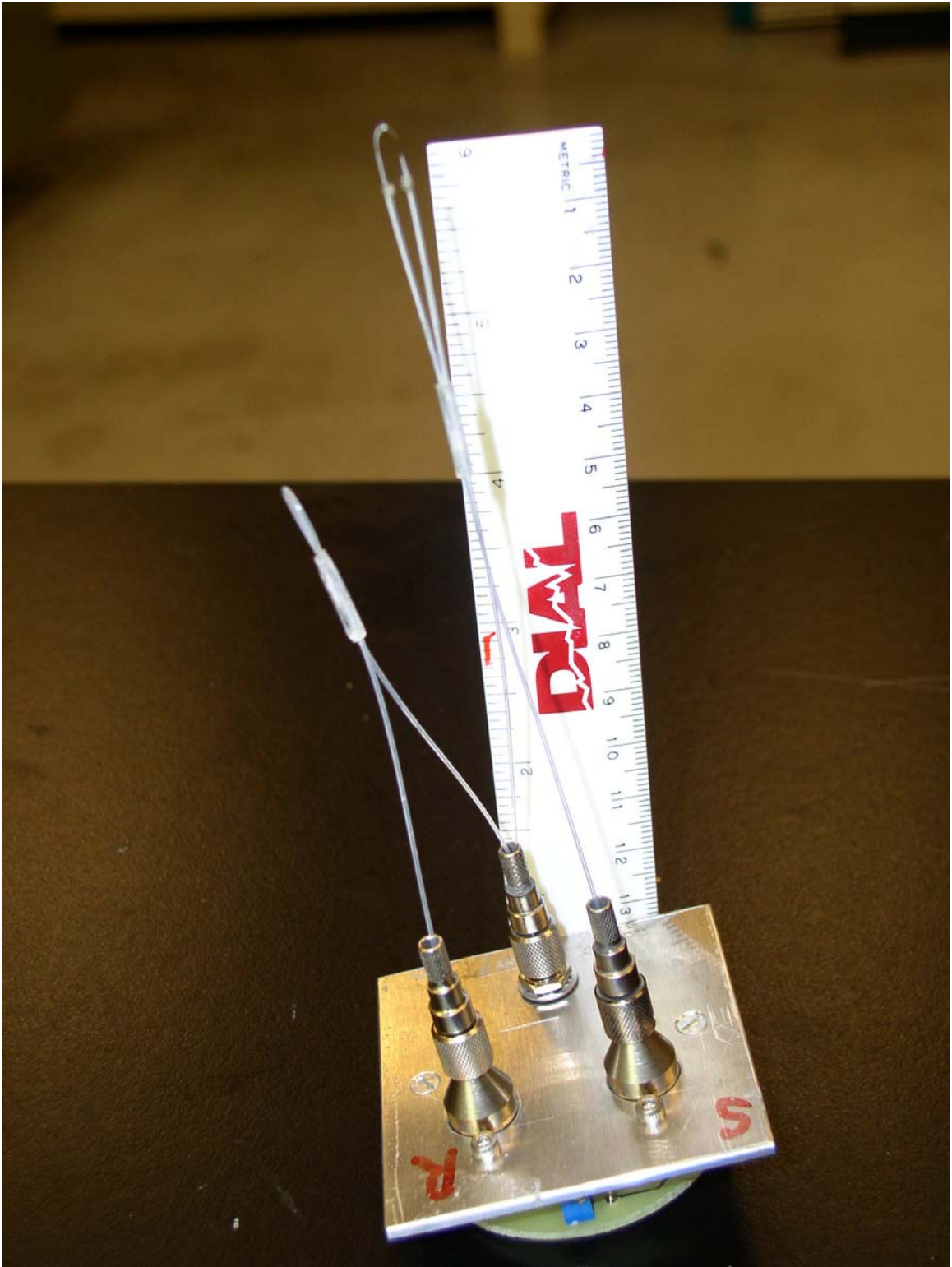


Figure 4.7 Top surface of the equipment.

CHAPTER V  
APPLICATIONS OF OPTICAL FIBER HUMIDITY SENSOR BASED ON  
EVANESCENT SCATTERING

**5.1 Application to soil moisture sensing**

*5.1.1 Soil moisture information needed*

Soil moisture information is valuable to a wide range of government agencies and private companies concerned with the weather, climate, soil erosion, reservoir management, waste tank management, geotechnical engineering, farmland irrigation, underground water resource exploration, etc. In almost all these applications, continuous monitoring of soil moisture is required.

*5.1.2 Problems of existing humidity sensors in sensing soil moisture*

Soil moisture sensors based on the detection of electric properties, such as dielectric constant or resistance, have been developed and commercialized. These sensors, however, suffer from the corrosive environment of soil. That is, the electrodes of these convenient sensors gradually corrode in soil, thus limiting their life-span. For most of the optical fiber humidity sensors discussed in Chapter 1, however, the stability of the reagent in the soil environment is an obstacle for wide acceptance of their application for soil moisture monitoring. In the gas phase inside soil, there are many chemical compounds such as ammonia, organic amine, hydrogen sulfide, etc. Some of these

compounds can react irreversibly with reagents doped in the polymer coating and deactivate the sensor permanently. In addition, some polymers or reagents can dissolve in water when the sensor is soaked in water for a long time, which happens in soil. Moreover, there are typically many dissolved chemicals in water when a soil sample is soaked in water. These chemicals can also irreversibly react with reagents or the polymer coating of the optical fiber sensors and deactivate the sensors.

### *5.1.3 Modification of sol gel silica coated bent probe*

The transducer of the current optical fiber sensor is only a thin layer of sol gel silica coating which is inert, stable and insoluble in water. Therefore, the sensor can still function properly after being soaked in water in extended periods of time, as shown in Figure 5.1. Between the first and second tests, the bent probe was soaked in water for ten days, between the second and third tests, the bent probe was soaked in water for ten days again. However, there are many-soluble compounds and colloid particles in soil water. These compounds and colloid particles can also be absorbed onto the surface of the sol gel silica and change the surface properties of the sol gel silica. Therefore, a protective coating, which is permeable to water vapor, but blocks out liquid water, is essential to isolate the sol gel silica coating from soil water. In an embodiment, silicone rubber was chosen as the protective coating material. Silicone rubber is highly permeable to water vapor and can block out the liquid water. After a silicone rubber protective coating was applied on the top of the sol gel silica coating, the resulting sensor can be used for long term soil moisture monitoring.

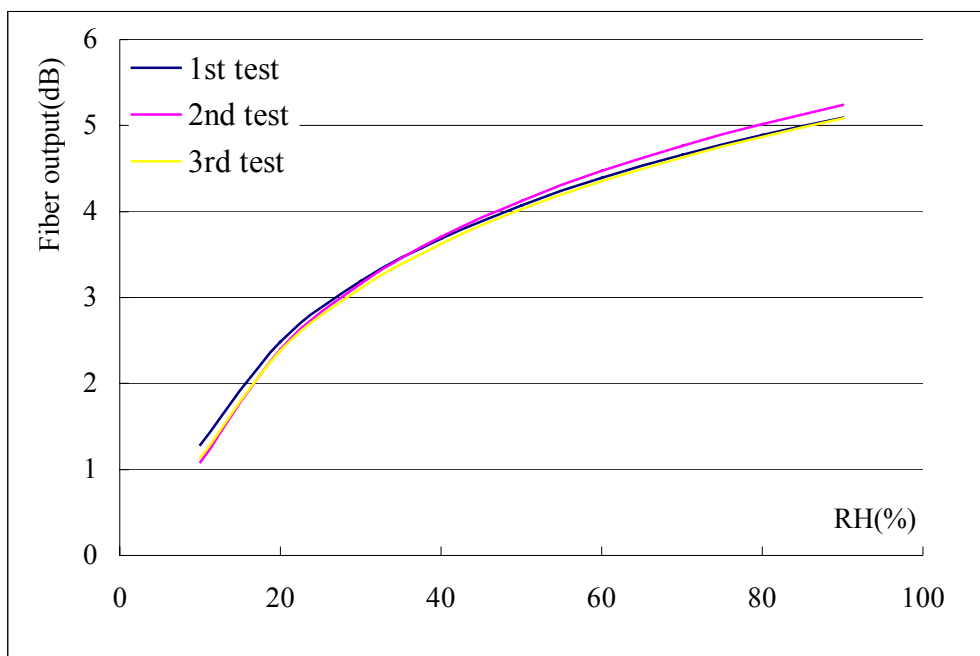


Figure 5.1 Calibration curves for sol gel coated probe test at different times. The probe was soaked in tap water between different test dates. During the tests, the bent probe was buried into soil sample in a flowerpot. The 2<sup>nd</sup> and 3<sup>rd</sup> tests are almost overlapped.

#### 5.1.4 Test and results

The sol gel silica coated optical fiber humidity sensor with silicone protective coating was tested with a dry soil sample in a flowerpot. The sensing signals of this sensor were monitored. Water was applied to the soil sample to slowly change its moisture content. Test results are shown in Figure 5.2. In this long-term test, the water content of soil was very high during some periods. However, the high water content did not affect the sensor. Therefore, the test result verified the capability of the sensor to be used for long-term soil moisture monitoring.

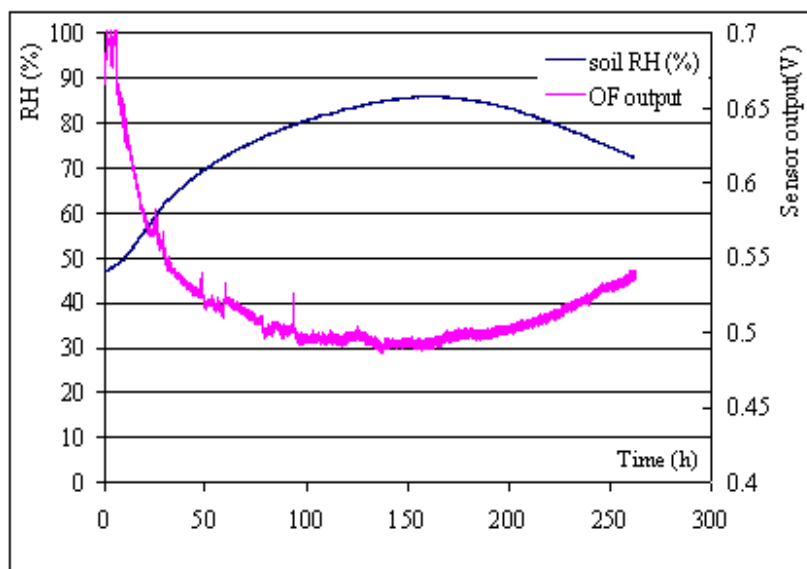


Figure 5.2 Long-term soil moisture monitoring using sol gel silica coated bent optical fiber sensor.

## 5.2 Application in concrete moisture sensing

### 5.2.1 Concrete moisture information needed

Concrete is the most widely used construction material in the world and is used in building, houses, bridges, roads, airport runways, etc. The strength and the stability of the concrete utilized are thus critical to the life-span of the constructed structure. The durability and any structural aging of concrete are governed by moisture content.

Water is at the heart of most of the physical and chemical causes underlying the deterioration of concrete structures. Among other effects, moisture levels determine the risk of corrosion attack occurring on cast-in steel and reinforcement and the rate of deleterious mechanism such as alkali-aggregation reaction. At the same time, a long aging-effect caused by drying-out of the cement matrix in concrete is evident, which

results in a reduced strength. A combination of dry and wet concrete may cause different shrinkage that in turn may well lead to cracking.

A balanced and stable moisture level would seem to be desirable, but cannot be achieved because the structural members are usually massive and are subject to different environments. In addition, concrete moisture content also affects the results of many tests concerning concrete properties. For example, moisture variation affects testing performance as the speed and penetration ability of acoustic and electromagnetic pulses used in modern techniques are strongly dependent on this factor. The criteria used in evaluating electrochemical test results are similarly affected by moisture. It may be said that any advance in non-destructive testing methods will be dependent on the ability to determine the moisture condition of massive concrete members on-site and the ability to use this information in processing measurement data.

### *5.2.2 Problems of existing humidity sensors for sensing the moisture content in concrete*

Detecting and monitoring moisture content in concrete structures is difficult with present sensing techniques. Two techniques — neutron meters and microwave measurements — have been proposed for detecting/monitoring moisture content in hardened concrete and are described by Bonin et al. [48] and Al-Qadi [49], respectively. The neutron technique involves radioactive material and therefore, its safety is a serious concern in its practical applications. The microwave technique is subject to serious matrix effect in concrete moisture detection. The detected signal from this method is affected by surface smoothness, air void content, concrete type, structure, *etc.*

Moisture sensors based on detecting electrical properties, such as capacitance and resistance, are inappropriate for concrete moisture monitoring because the electrode of sensor can corrode in the corrosive environment inside the concrete. In addition, the sensing element of these electrical property-based sensors normally cannot survive in the high alkalinity cement mortar.

### *5.2.3 Modification of sol gel silica coated bent probe*

The humidity sensor for monitoring the moisture content in concrete has the same structure as that used for air humidity sensing. In order to protect the sensing element from damaging by high alkaline mortar during sensor deployment, the bent probe is sealed with a round button microporous ceramic tube which isolated the bent probe from the alkaline mortar and allows water molecules to pass through it.

### *5.2.4 Test and results*

This ceramic tube packed bent probe was then buried inside a concrete block at the time of making the concrete block from cement. After the concrete hardened, the concrete block was put into a gas sealed plastic box with gas inlet and gas outlet ports opened on the wall of the box as shown in Figure 5.3.

As the concrete was drying, the bent probe guides more light to the detector and sensor's output signal (in voltage) increases with time, as shown in Figure 5.4. After more than 50 hours, the moisture content inside the concrete block equilibrated with the moisture content in the air and the output signal of the sensor stabilized. After more than 10 days, the dry-air flow stopped, and 30ml water was added into the box. The concrete block absorbed water and moisture content inside the concrete increased. The output

signal of the sensor in voltage decreased. The test results in Figure 5.4 show that the sensor can be used for applications of monitoring moisture content in concrete structures.

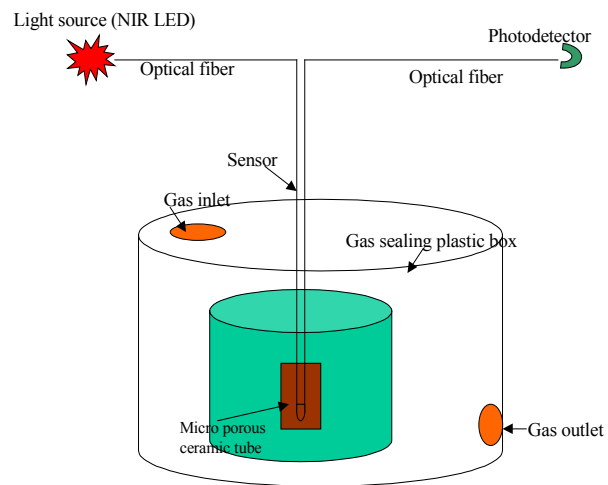


Figure 5.3 Experiment setup for long-term monitoring the moisture in concrete

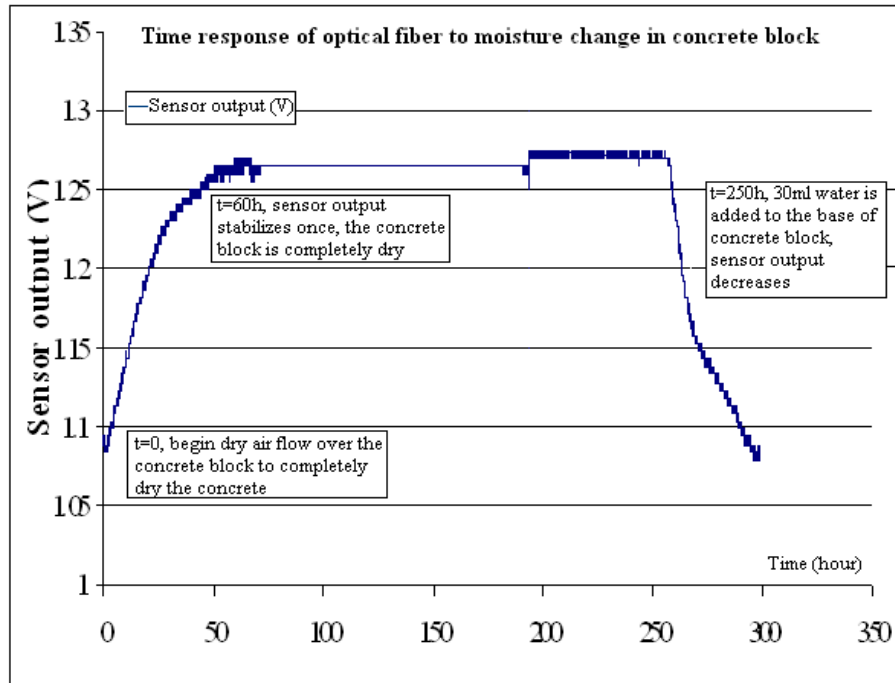


Figure 5.4 Time response of optical fiber sensor to monitor moisture changes in concrete block. For clearness in the graph, the straight line inside demonstrates stable output during long term test under same relative humidity environment.

## CHAPTER VI

### SUMMARY OF PROTOTYPE OPTICAL FIBER HUMIDITY SENSOR

The evanescent wave scattering has been used to design an optical fiber humidity sensor. The advantages of this sensor includes simple structure, low cost, small size, fast response, reversibility, wide dynamic range, high sensitivity and stability. According to our knowledge, this is the first optical fiber sensor having the capability to detect water vapor in air gas down to low ppm levels. Several applications of this humidity sensor were presented. Potentially, this sensor and the technique, which is based on evanescent wave scattering phenomenon occurring in sol gel silica coating, can be applied to many areas.

## REFERENCES

- [1] Andy Bailey, Gary Palmer,  
<http://ces.ca.uky.edu/darktobacco/pubs/green%20TOBACCO3.pdf>
- [2] J.R Kokan, R.A Gerhardt, <http://www.synaps-inc.com/PDF/sensorpaper.PDF>
- [3] H. Aust, M. Oerder, F. Seide, and V. Stenbiss, *Speech Communication*, vol. 17, Nov. 1995, pp. 249-262.
- [4] Jian Wu, Jan Suls and Willy Sansen, *Analytical Sciences*, 15, 1029(1999)
- [5] K.T.V.Grattan and Dr.T.Sun, Elsevier Science, sensor and actuators 82,pp 40-61 (2000)
- [6] Eric Udd, SPIE- International Society for Optical Engineering (1986)
- [7] Tae Young Kim; S.K.S; J.H.N; T.T, *Dielectrics and Electrical Insulation*, Vol.10, Issue 2, April, 2003, 266-270
- [8] Newby,K; Reichert, W.M; Andrade, J.D; Benner, R.E. *Appl. Opt*, 1984, 23, 1812-1815
- [9] Ballantine, D.S; Wohltjen, H. *Anal.Chem.* 1986, 58, 2883-5.
- [10] Zhou, Q; Shahriari, M.R; Kritz, D; Siegel, G.H, Jr. *Anan Chem*, 1988, 60, 2317-20.
- [11] Nevergold, M.W; Abel, K, *Spectroscopy* 1990, 5, 46-8.
- [12] Boltinghouse, F; Abel, K, *Anal Chem*, 1989, 61,1863-6
- [13] Wang, K; Seiler,K; Huang, J.P; Lehmann, B; West, S; Hartman, K; Simon, W. *Anal Chem*, 1991,63, 970-4.
- [14] Morisawa, M; Uematsu, H; Muto, S. *Jpn.J. Appl.Phys*, 1992, 31, L1202-5.
- [15] Sadaoka, Y; Matsuguchi, M; Sakai, Y; *Sens. Actuators A*1991,25-7, 489-92.

- [16] Sadaoka, Y; Matsuguchi, M; Sakai, Y; Murata, Y, Sens. Actuators B 1992, 7, 443-6.
- [17] Sadaoka, Y; Matsuguchi, M; Sakai, Y; J. Electrochem. Soc. 1991, 138,614-5.
- [18] Sadaoka, Y; Matsuguchi, M; Sakai, Y; Murata, Y, Chem. Lett, 1992, 53-6.
- [19] Sadaoka, Y; Matsuguchi, M; Sakai, Y; Murata, Y, J.Mater.Sci, 1992, 27,5095-100.
- [20] Zhu,C; Bright,F.V; Wyatt,W.A; Hieftje, G.M.J.Electrochem.Soc, 1989, 136, 567-70
- [21] Mitschke, F. Opt. Lett, 1989, 14, 967-9.
- [22] Kunz, R. E. Sens. Actuators B 1993, 11, 167-76.
- [23] Otsuki. S; Adachi. K. Anal. Aci. 1993, 9, 299-301.
- [24] Jindal,Rajeev; Tao,Shiquan; Singh,jagdish P; Gaikwad,Parikshit, SPIE ,vol 4578, 314-319
- [25] Shiquan Tao, Christopher B, Winstead, Raheev Jindal, Jagdish P.Singh, IEEE sensors J, Vol 4,June 2004, 322-328
- [26] Avnir, D; Levy, D; reisfield, R.J,J.Phys.Chem, 1984, 88, 5956-5959
- [27] Lev, O; Tsionsky, M; Rabinovich,L; Glezer, V; Sampath,S; Pankretov, I; Gun, J.Am.Chem.Soc, 1995, 67,22A-30A
- [28] Brinker, C.J; Scherer, G.W. Sol-gel Science; Academic Press, Inc; Sandiego, 1990
- [29] Dave,B.C; Dunn,B; Valentine,J>S.Anal.Chem. 1994, 66, 1120-1127
- [30] McCormick A. Sol-gel processing and applications, Attia, Y.A, Ed; Plenum Press: New York, 1994, 3-15
- [31] Hoffman, P *Angewan. Chem.* 1934, p 539-558

- [32] L.E. Scriven, Physics and applications of dip coating and spray coating, in *Better Ceramics through Chemistry*, □, C.J.Brinker,D.E. Clark and D.R.Ulrich, *Mater. Res. Soc.*, Pittsburgh, PA, 1988,717-729
- [33] L.D. Landau and B.G.Levich, *Acta Physiochim.* U.R.S.S, 17 (1942) 42-54
- [34] C.J.Brinker, G.C. Frye, A.J. Hurd and C.S.Ashley, Fundamentals of sol-gel dip coating, *Thin Solid Films*, 201 (1991) 97-108
- [35] C.J. Brinker, A.J Hurd, P.R. Schunk, G. C. Frye and C.S. Ashley, review of sol-gel thin film formation, *J. Non-Cryst. Solids*, 147&148 (1992) 424-436
- [36] D. E. Bornside, C. W. Macosko, L. E. Scriven, On the modeling of Spin coating, *J. Imaging Techn.*,13, 122 (1987)
- [37] Xiancai Fu, Wenxia Shen, Tianyang Yao, *Physical Chemistry*,1995, 942
- [38] M.R. Shahriari, optical fiber sensor technology, Vol. 4, 1998, Kluwer Academic Publishers, London.
- [39] Ellerby, L.M.; Nishida, C.R.; Nishida,F.; Yamanaka,S.A.; Dunn,B; valentine, J.S.; Zink, J.I. *Science* 1992, 255, 1113-1115.
- [40] Kuselman, I.; Kuyavskaya, B. I.; Lev, O.*Anal. Chim.Acta* 1992, 256, 65-68
- [41] G.E. Badini, K.T.V.Grattan, A.W. Palmer and A.c.c.Tseung, Springer Proc. In Physics, Springer, Berlin, Heidelberg, 44 (1989)436-442.
- [42] Ding, J.Y.;Shahriari,M.R.; Sigel,G.H.*Electron.Lett*, 1991,27,17,1560-1562.
- [43] Khijwania,S.K.; Gupta, B.D., *Optics Communications*, Volume 175, Issue 1-3, 135-137.
- [44] S.Kassam, A.Duparre, K.Hehl, P.Bussemer, and J.Neubert, *Applied Optics*. 31,1304-1313 (1992)
- [45] Langley et al., *Experimental methods in the physical science*, Vol. 35, 263-300.
- [46] T.V.Oommen, Electrical Electronics Insulation Conference, 1991. Boston '91 EEIC/ICWA Exposition., Proceedings of the 20<sup>th</sup>

- [47] S.M. Fine, R.M. Rynders and J.R. Stets J. Electrochem. Soc., Vol. 142, No. 4, April 1995
- [48] Nuclear Technology, 95(3), 337-348(1991).
- [49] Testing and Evaluation, 21(1), 43-50(1992).